UNIVERSITY OF CAPE TOWN

DEPARTMENT OF HUMAN BIOLOGY:

BIOMEDCIAL ENGINEERING

TOWARDS IMPROVED VISUAL STIMULUS DISCRIMINATION IN AN SSVEP BCI

SUMBITTED TO THE UNIVERSITY OF CAPE TOWN IN PARTIAL FULFILMENT OF THE REQUIREMENTS FOR THE DEGREE:

MSC MED IN BIOMEDICAL ENGINEERING

AUTHOR: DEAN LESLIE HODGSKISS

SUPERVISOR: DR LESTER JOHN

SUBMITTED: FEBRUARY 2010

Declaration

I declare that this thesis is my own, unaided work. Where any information has been drawn from other sources, I believe that the text has been suitably referenced. This thesis has not been submitted before for any degree or examination at any university.

Dean Hodgskiss

Cape Town, February 2010

Abstract

The dissertation investigated the influence of stimulus characteristics, electroencephalographic (EEG) electrode location and three signal processing methods on the spectral signal to noise ratio (SNR) of Steady State Visual Evoked Potentials (SSVEPs) with a view for use in Brain-Computer Interfaces (BCIs). It was hypothesised that the new spectral baseline processing method introduced here, termed the 'activity baseline', would result in an improved SNR. Furthermore it was also hypothesised that the use of vertical oriented stimuli would prove to have greater SNR than that of horizontally orientated stimuli.

Nine participants were seated in a chair in a darkened room and viewed combinations of SSVEP inducing stimuli presented on a PC monitor. EEG recording electrodes were placed on locations PO_7, O_1, O_Z, O_2 and PO_8. The visual stimulus frequency was varied from 8 to 20 Hz and the shapes were horizontal and vertical lines and rectangles and square checks. Three different spectral baselines were used: the standard 'eyes open' and ‘eyes closed’ baseline, and a novel 'activity baseline'.

Custom EEG electrodes were designed and built for the study. SSVEP data was acquired using open source hardware (OpenEEG) and open source C++ software (BrainBay). EEG signal processing and statistical analysis was carried using Matlab and R.

By applying a linear mixed effects model to the data, the results predicted with a high level of significance that an activity baseline would achieve a greater SNR across all electrodes and certain frequencies, and specifically where alpha band noise was involved. The SNR response to different shapes was predicted to follow the discharge rates of single neurons in V4 as described in the literature, except for a vertical stimulus, which may or may not have performed badly due to adaptation characteristics. Thus, square checks generally had the largest SNR followed by vertical rectangles.

In conclusion, the activity baseline significantly improved the SNR and may thus be used to advance the state of art of SSVEP BCIs.

Acknowledgements

To Dr. Lester John, my supervisor, thank you for the support and advice over the years. It has been invaluable to me. Your support in securing funding and initiating my visit to Graz among all the other things are much appreciated.

Prof. Kit Vaughan and the MRC/UCT Medical Imaging Research Unit as a whole for funding and support

Dr. Lize van der Merwe, your help with the statistics and vast input on my write up of the results was crucial and much appreciated.

Thank you to Prof. Pfurtscheller and the team in Graz for support and direction.

Thank you to my Mum for her enduring support, without which I would have not completed this degree.

I'd like to acknowledge my Dad for first planting the seeds of Maths and Science and encouraging it through my childhood.

To Dr. Fleur Howells, my buddy, thanks for the friendship and the spur lunches.

The National Research Fund for funding received.

Thanks to my Ilsie for your love.

Table of Contents

1 INTRODUCTION 1

2 BACKGROUND BCI LITERATURE 3
2.1 Electroencephalography (EEG) and Its Place In BCIs 3
2.2 Design Of An EEG-Based BCI 5
2.2.1 Electrodes and Amplifiers 6
2.2.2 Feature extraction 6
2.2.3 Translation Algorithms 7
2.2.4 Control Interface 9
2.3 Types Of EEG-Based BCIs 9
2.3.1 Dependent and Independent BCIs 9
2.3.2 Neurophysiological Signals used in BCIs 10
2.3.3 Slow Cortical Potentials 10
2.3.4 P300 Evoked Potentials 11
2.3.5 Mu and Beta Rhythms 12
2.3.6 Visual Evoked Potentials 14

3 NEUROPHYSIOLOGY OF THE HUMAN VISUAL SYSTEM 17

4 SSVEP LITERATURE REVIEW 23
4.1 Stimulus Parameters 23
4.1.1 Temporal Frequency 23
4.1.2 Colour and luminance 26
4.1.3 Size of stimuli 27
4.1.4 Spatial Frequencies 28
4.1.5 Direct and Covert Attention 30
4.1.6 Type of stimulus: Checkerboard vs flicker 31
4.2 Visual Feedback 31
4.3 Adaptation Characteristics 32
4.4 Electrode Placement 33
4.5 Baseline 35
4.6 Signal To Noise Ratio 35
4.7 Other Considerations 35

5 OBJECTIVE OF INVESTIGATION 37
5.1 Critique Of Literature 37
5.2 Aim 37
5.2.1 Investigation of an activity baseline to reduce background EEG 37
5.2.2 Investigation of the effect of shapes on the SSVEP 37

6 METHODOLOGY 39
6.1 Experimental Setup 39
6.1.1 Shape of Stimuli Experiment 40
6.2 Analytical Methodology 42
6.2.1 Unpacking of Data 42
6.2.2 Measure to counteract correct phase change from freezing stimulus 42
6.2.3 The FFT and rendering of Data 43
6.2.4 SNR 43
6.2.5 Calculation of Resting and Activity Baselines 43
6.2.6 Statistical Analysis 44
6.3 Towards A Real-Time BCI 46

7 RESULTS 49
7.1 Main Effects 51
7.1.1 Baselines 51
7.1.2 Shapes 52
7.1.3 Electrodes 52
7.1.4 Frequency 53
7.2 Interaction Effects 54
7.2.1 Baseline:Frequency Interaction 54
7.2.2 Baseline:Electrode Interaction 55
7.2.3 Shape:Frequency Interaction 56

8 Discussion 59
8.1 Main Effects 59
8.1.1 Activity Baseline 59
8.1.2 Shapes 60
8.1.3 Electrodes 60
8.1.4 Frequencies 60
8.2 Interaction Effects 61
8.2.1 Baseline:Frequency Interaction 61
8.2.2 Baseline:Electrode Interaction 61
8.2.3 Shape:Frequency Interaction 61

List of Figures

Figure 1. Top and side views illustrating the international 10-20 positioning system. The letters F, C, T, P and O stand for Frontal, Central, Temporal, Parietal and Occipital respectively. The distances between electrodes are typically 10 or 20 % of a half head circumference apart. For instance, Fp is 10% from the Nasion and 20% from Fz. Similarly O1 and O2 are 10% from Oz (loki23, 2010; BCI2000, 2010)..... 4

Figure 2. Basic design and operation of a BCI system. Electrical signals of the order of µV are acquired from the scalp, amplified and digitized. The BCI then extracts features of interest which are classified into device commands for the interface with the user (Wolpaw *et al*, 2002). 5

Figure 3. The excitement in the power spectrum at 12 Hz and its corresponding 2nd harmonic of 24 Hz is easily discernable and can be identified by using a threshold line for unusually high activity. 8

Figure 4. A typical time domain representation of a slow cortical potential. The dotted line is associated with relaxation, while the solid line is associated with cortical activation. (Wolpaw *et al.*, 2002) 10

Figure 5. The P300 response is associated with an amplitude increase approximately 300 ms after a stimulus, as seen here in the time domain. (Wolpaw *et al.*, 2002)..... 11

Figure 6. In the frequency domain a peak in the mu range of frequencies is indicative of movement imagery over the motor cortex. (Wolpaw *et al.*, 2002)..... 12

Figure 7. A sagital view of the cortex with an Homunculus indicating areas of the motor cortex relating to movement (Poulin, 2008)..... 13

Figure 8. Reversing checkerboards of different frequencies allow a BCI user to move the bar on the bottom of the screen left and right to prevent a bouncing orange ball from falling through the bottom of the window. This setup was developed by the author and was played by visitors to the 2004 Department of Science and Technology Exhibition in Sandton, Johannesburg. 14

Figure 9. High level axial overview of the human visual system (Kandel *et al*, 2000) 17

Figure 10. Transverse view of the human visual system with particular attention to the layers of the lateral geniculate nucleus (Kandel *et al*, 2000) 18

Figure 11. Different areas in the primary visual cortex process information from different parts of the visual field (Kandel *et al*, 2000). 19

Figure 12. Neurons in V4 have optimal discharge rates for circular stimuli, and vertical stimuli have a higher rate than horizontal (Kandel *et al*, 2000)..... 20

Figure 13. PET images indicate activity around electrodes PO_7 and PO_8 related to moving stimuli and therefore motion processing (Kandel *et al*, 2000). 21

Figure 14. Amplitude of SSVEP response is separated into 3 subsystems (Regan, 1989) 24

Figure 15. Graphical representation of the relative sensitivity of the human eye to different colours (nikondigital, 2010). 26

Figure 16. Black and white, and red and green checkerboards have different effects on harmonics of stimulation frequencies 27

Figure 17. 4 checkerboards with increasing spatial frequency from left to right 28

Figure 18. The angle subtended by a stimulus is computed from the size of the stimulus and the subject's distance from the stimulus. 29

Figure 19. Subjects presented with 20 second duration trials for both 6 (left) and 10 Hz (right) stimuli experienced an initial stimulation period peaking at 6-7 trials whereafter there was an amplitude decline (Beverina *et al*, 2003). 33

Figure 20. A 6 lead modularEEG comprising 3 analog amplifier boards on the left and 1 digital board on the right. 39

Figure 21. SSVEP experimental setup. A subject attends the stimulus on the computer monitor. EEG electrodes which have been developed in the laboratory by the author are attached to the custom-made elastic electrode band such that the electrodes are at PO7, O1, Oz, O2, and PO8. 40

Figure 22. Stimuli presented to subjects are reversing boards with horizontal and vertical lines, horizontal and vertical rectangles, and checks, all of the same width. 41

Figure 23. Matlab processing of data is represented in a block diagram. 42

Figure 24. Both the closed-eyes and open-eyes baselines show pronounced alpha activity. The activity baseline has a much reduced alpha while it shows peaks at the stimulation frequencies of 8, 10, 12, 15 and 20 Hz since it is an average of all the trials when a subject was attending stimuli 44

Figure 25. When the total data across all subjects (left) was logged it was found to have a closer to normal distribution (right) 45

Figure 26. The brainbay setup on the left is made up of functional boxes which are connected by wires. In this way a number of processing algorithms can be programmed independently and then used in series or parallel to test efficacy of individual algorithms or combinations thereof. The author modified the program to enable it to process data in the frequency domain and as such be able to operate as an online SSVEP BCI such as the game on the right hand side and figure 8. 47

Figure 27. The activity baseline will perform better at 10 and 20 Hz 54

Figure 28. The predicted values expect the activity baseline to perform better across all electrodes, while the eyes-closed baseline is expected to perform the worst. 55

Figure 29. Different shapes over frequency reveal that vertical rectangles are expected to perform best over the majority of the frequencies 57

Figure 30. Illustration of concept that may describe the interaction between Frequency and Shapes 57

List of Tables

Table 1. Difference in sensitivity of M and P cells to stimulus features (Kandel *et al*, 2000)..... 19

Table 2. ANOVA table for final model..... 49

Table 3. Summary of fixed effect estimates from final model. 50

Table 4. Predicted values of the baselines when effects of all other factors have been stripped away. Activity baseline is predicted to have the superior SNR. 51

Table 5. Predicted values of the shapes when effects of all other factors have been stripped away. Vertical rectangles follows checks as the 2nd highest predicted SNR..... 52

Table 6. Predicted values of the electrodes when effects of all other factors have been stripped away. O_Z which is situated over the primary visual cortex had the highest estimated SNR. 53

Table 7. Predicted values of the frequencies when effects of all other factors have been stripped away. 53

Table 8. Logged values showing the individual interaction SNRs of frequency and baseline where all effects of other factors have been stripped away 55

Table 9. Unlogged values showing the individual interaction SNRs of frequency and baseline ... 55

Table 10. Logged values showing the individual interaction SNRs of electrode and baseline where all effects of other factors have been stripped away 56

Table 11. Unlogged values showing the individual interaction SNRs of electrode and baseline .. 56

Table 12. Logged values showing the individual interaction SNRs of frequency and shape where all effects of other factors have been stripped away 58

Table 13. Unlogged values showing the individual interaction SNRs of frequency and shape 58

1 Introduction

The state of being a healthy brain locked in a body incapable of movement, with severely compromised ability to communicate one's thoughts to the outside world is aptly described in THE DIVING BELL AND THE BUTTERFLY by Jean-Dominique Bauby. This memoir was written by Jean-Dominique after having suffered a brainstem stroke at the age of 43, robbing him of all neuromuscular control save for eye movement. He communicated his thoughts by blinking to a nurse every time the pointer she was holding ran across the appropriate letter on an alphabet board.

As can be imagined, this was painfully slow, and particularly heart-breaking to try to communicate to his two young children. Jean-Dominique took 18 months to complete the book on his experiences, and through this painstaking struggle left an amazing work testifying to his love for his family, his resilience and courage, and the extreme emotional challenges that people in his position find themselves. Thankfully Jean-Dominique's and others' plight has not gone unseen by the scientific world and there is a growing body of researchers; scientists, engineers, healthcare professionals and others; who explore ways in which the lives of locked-in people like Jean-Dominique may lead more comfortable, dignified, and productive lives.

Individuals that are 'locked-in' are conscious and lucid, but have lost the ability to communicate with the external environment as their muscular motor units do not receive the required neural information to facilitate movement. Locked-in syndrome can have a number of causes:

- Traumatic brain injury
- Diseases of the circulatory system
- Medication overdose
- Damage to nerve cells, particularly destruction of the myelin sheath, caused by disease (e.g. central pontine myelinolysis secondary to rapid correction of hyponatremia).
- Stroke or brain haemorrhage

In all of the abovementioned cases patients will at some stage need an intervention in order to communicate with those around them. It is in part to satisfy this need that Brain-Computer Interfaces (BCIs) of different kinds, based on different kinds of neural signals, continue to be developed.

2 Background BCI Literature

The Brain Computer Interface (BCI) is an apparatus that provides a communication channel directly from the brain. This communication channel makes use of little or no neuromuscular functionality, and so has the potential to provide locked-in people with a means of interacting with the outside world.

2.1 Electroencephalography (EEG) and its place in BCIs

There are a number of ways to gain information from brain activity for BCIs, but Electroencephalography (EEG) has been chosen for the purpose of this study. EEG has historically, in terms of volume of research, been favoured above MEG, PET, fMRI and optical imaging applications of the BCI (Wolpaw *et al.*, 2002). This is most likely due to it being relatively inexpensive, easy to employ practically, and suited to rapid BCI communication. The superior speed is as a result of most of these other modalities depending on blood flow which has long time response constants to BCI stimuli, whereas the electrical response measured by EEG is much faster.

EEG involves the acquisition of electrical signals from a person's scalp by means of electrodes which have been applied non-invasively. These signals are generated by neurons and groups of neurons in the brain, and as such provide some indication of brain activity.

The number of electrodes used for EEG can vary according to the application, where the use of many electrodes is known as high-resolution EEG (up to 256 electrode systems are available commercially) and few electrodes as low-resolution EEG. For BCI studies electrode positions for obtaining specific neural information have often been clearly defined in previous literature, and so generally the EEG used in BCIs is low-resolution. Standard EEG electrode positions have been defined by the 10-20 international positioning system so that EEG studies can be better compared according to underlying brain structures. The position names are based on the underlying structures and distances between electrodes are generally 10 or 20 percent of a half-head circumference from each other. Figure 1 illustrates some of the positions used in the 10-20 system.

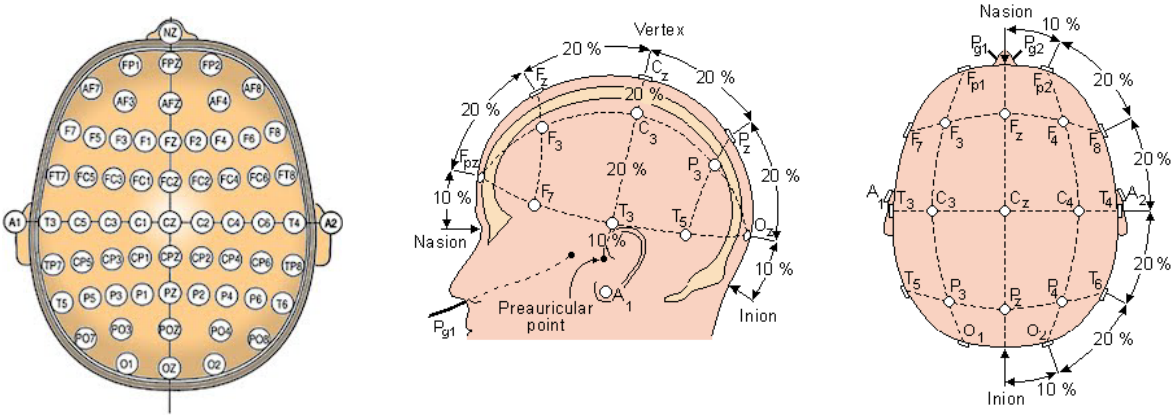

Figure 1. Top and side views illustrating the international 10-20 positioning system. The letters F, C, T, P and O stand for Frontal, Central, Temporal, Parietal and Occipital respectively. The distances between electrodes are typically 10 or 20 % of a half head circumference apart. For instance, Fp is 10% from the Nasion and 20% from Fz. Similarly O1 and O2 are 10% from Oz (Loki23, 2010; BCI2000, 2010)

A major drawback of EEG is that the resolution and reliability of the information detectable in the spontaneous EEG is limited by a number of factors including:

- the vast number of electrically active neuronal elements (>100 billion),
- the complex electrical and spatial geometry of the brain and head,
- the trial-to-trial variability of brain function.

Thus, the possibility of recognizing a single message or command amidst this complexity has until recently appeared remote.

With the extremely rapid and continuing development of inexpensive hardware, however, sophisticated online analyses of EEG have become possible. Scientists have employed a vast number of signal processing techniques, some better than others, to extricate relevant EEG features for BCI communication.

The use of BCIs has in fact been proven in quantitative studies to be quite realisable with most people (Guger *et al.*, 2009; Allison *et al*, 2010). Practical applications already realised include various spelling programs (Birbaumer *et al*, 1999; Millan and Mourino, 2003; Wills and Mackay, 2006; Nijboer *et al.*, 2008), Mouse cursor control (Trejo *et al*, 2006), wheel-chair control (Leeb *et al*, 2007) and a mind-controlled functional electrical hand stimulation in a quadriplegic (Pfurtscheller *et al.*, 2003).

2.2 Design of an EEG-based BCI

Since BCI research is a multi-disciplinary field integrating neuroscience, psychology, engineering, computer science, and others, there have been several varied approaches to the design of BCI systems (Mason and Birch).

As per Wolpaw *et al* (2002), a BCI has inputs (in this case EEG signals), outputs (device commands or communication activities), components that translate input to output, and a protocol that determines the onset, offset, and timing of operation. Figure 2 is a basic representation of the components of an EEG BCI.

The functional components that translate the input to output in an EEG BCI are the electrodes, amplifier, feature extractor, feature translator and the control interface as illustrated in figure 2.

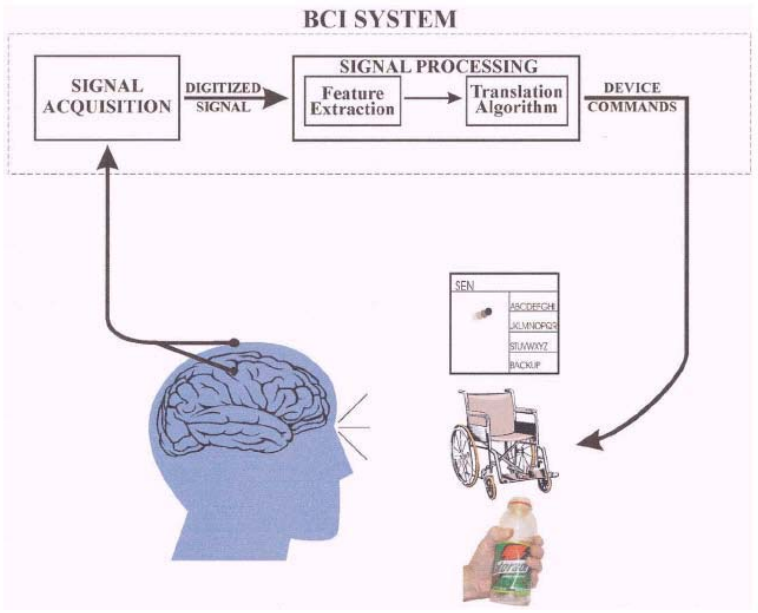

Figure 2. Basic design and operation of a BCI system. Electrical signals of the order of µV are acquired from the scalp, amplified and digitized. The BCI then extracts features of interest which are classified into device commands for the interface with the user (Wolpaw *et al*, 2002).

2.2.1 Electrodes and Amplifiers

The role of the electrodes and amplifiers is to convert the user's ionic electrical activity into electrical signals and then to amplify and digitize these signals.

Electrodes are either active or passive, based on whether or not they have unity gain amplifiers close to the electrode, and these tend to be based on capacitive or ionic transfer respectively. Both types of electrodes were successfully developed in the laboratory by the author, but for the purpose of this study only the passive electrodes were used. See appendix A for more information on EEG electrodes and those developed in the laboratory.

Since EEG signals are of the order of µV, amplifiers for EEG purposes amplify by a gain of around 10^6. The signals are digitized at 10 bits or more to maintain fidelity of the signal, but information transfer can be at a relatively low rate (a few hundred Hz) because EEG frequencies of interest are generally below 50 Hz due to the low-pass filter characteristic of the skull on brain activity (Teplan, 2002). In particular, the 2 well established types of EEG BCIs which rely on the frequency domain are concerned with the ranges of 8 to 30 Hz and 6 to 40 Hz (Wolpaw *et al*, 2002). These BCIs will be discussed in more detail in section 2.3.5 and 2.3.6.

2.2.2 Feature extraction

Feature extraction is the process by which the signal to noise ratio (SNR) of the neural activity is greatly increased in order to make the information more meaningful to the BCI.

In more technical terms, the digitized signals received from the amplifier are transformed by the feature extractor into feature values that correspond to the underlying neurological event used to control the BCI. To be consistent with the pattern recognition community this is referred to as a 'feature vector' (Fukunaga, 1990).

The feature vector is realized by subjecting the digitized signal to one or more of a number of feature extraction procedures such as baseline subtraction, spatial filtering, amplitude averaging, or spectral analyses. One of the primary focuses of this thesis is baseline subtraction, where typically a baseline is

obtained from a subject's resting EEG which is then compared to active EEG (EEG activity while a user is controlling a BCI) in order to increase the SNR. This is elaborated upon in section 5.1 and 5.2.1.

BCIs can use signal features that are in the time domain (e.g. evoked potential amplitudes) or the frequency domain (e.g. alpha, mu or beta-rhythm amplitudes) and could conceivably even use both, thereby improving performance (Schalk *et al*, 2000; Blankertz *et al*, 2003; Parra *et al*, 2003). Section 2.3 is an overview of the most common types of EEG BCIs.

Whether in the time or frequency domain, the first step of a feature extractor is typically to band pass the data. This means to exclude signals that have a frequency higher or lower than those that are of interest for the BCI application. The lowest frequency that is usually excluded is anything less than 0.5 Hz since this is tending towards DC which is too slow for a BCI and is susceptible to movement noise. Frequencies of less than 40 Hz are of interest (see 2.2.1).

Further feature extraction is usually specific to the type of EEG BCI being employed, and this would be dependent on the nature of the brain activity being used to drive the BCI. For example, certain brain activity is localized to a particular part of the brain, and in this case spatial filtering would increase the SNR, while other activity used in certain BCIs is found over much of the cortex.

In a many types of BCIs, features are specific to a user, and as such training would be required to allow the feature extraction algorithm to be tailored to the feature of interest. This factor makes it very difficult to have a plug and play feature extractor for any user. This is one of the reasons the author has chosen to focus on a steady state visual evoked potential (SSVEP) BCI which requires no training. The SSVEP BCI is introduced in 2.4.6.

2.2.3 Translation Algorithms

BCI translation algorithms convert the extracted signal features into control commands. Also known as feature classification, there is a wealth of literature concerning the development of algorithms for BCIs (and the use of algorithms developed elsewhere and applied to BCIs).

One of the simplest methods is known as thresholding, and will be used as an illustrative example. If a feature vector is known to be say a peak at the 12 Hz frequency, a thresholding translation algorithm would monitor the amplitude or power of this specific frequency in the frequency domain. A specific magnitude would be decided upon as the threshold, and if the amplitude or power were greater than this threshold at any one time, the algorithm would indicate to the control interface that the user has signaled an intention related to the feature measured.

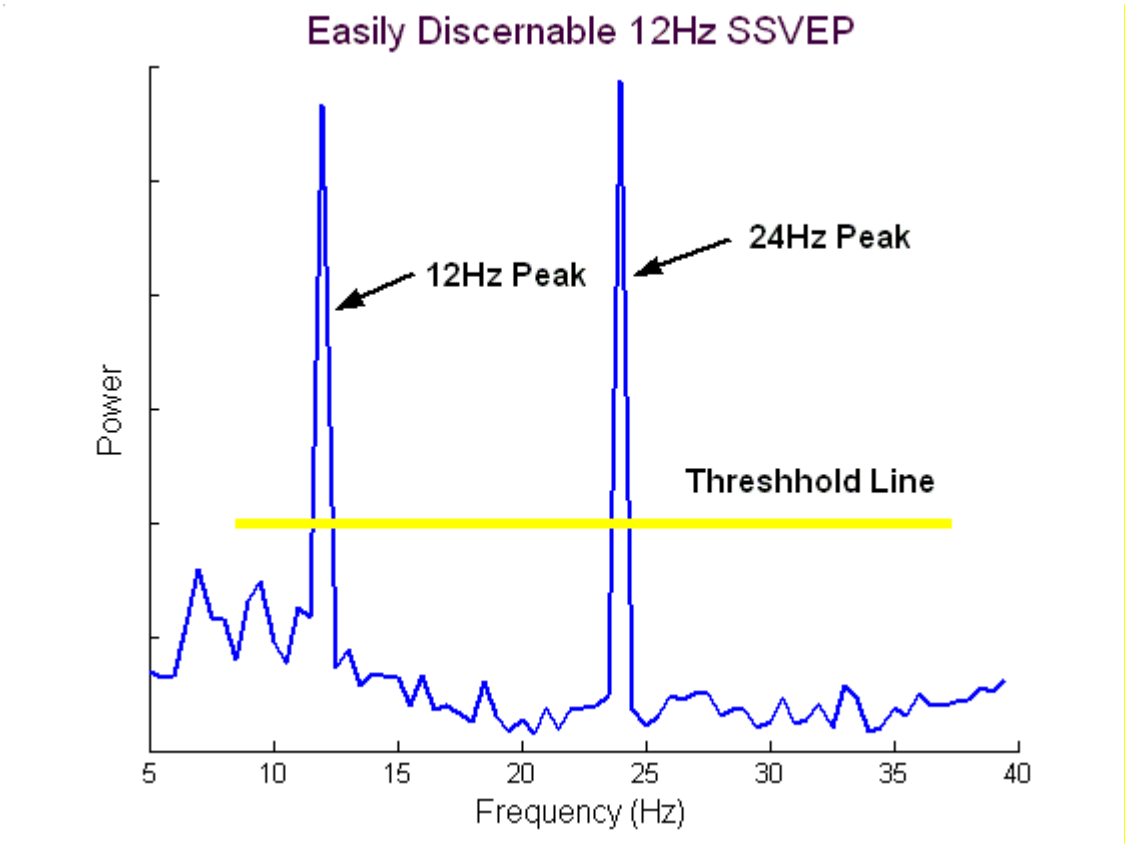

Figure 3. The excitement in the power spectrum at 12 Hz and its corresponding 2nd harmonic of 24 Hz is easily discernable and can be identified by using a threshold line for unusually high activity.

Since this dissertation is not concerned with translation algorithms of BCIs, and it is a vast topic and difficult to provide objective comparisons between methods, the author advises the reader to consult a review article by Bashashati *et al* (2007) for further information.

2.2.4 Control Interface

The control interface translates the logical control signals from the feature translator into signals that are appropriate for a particular type of device or some kind of communication. It will vary greatly depending on the environment and the specific application of the BCI. A good example of a control interface for a BCI is DASHER (Wills and Mackay, 2006) which has a predictive spelling and grammar function which aids a subject in spelling words faster.

2.3 Types of EEG-based BCIs

2.3.1 Dependent and Independent BCIs

In certain types of BCIs limited muscular control is necessary for a subject to select from a number of options presented by the BCI. The muscular control used is normally eye movement which is often still present in locked-in individuals.

When eye movement is necessary, the BCI is termed 'dependent'. For example, one BCI presents a user with a selection of targets on a computer screen that flash at different frequencies, and the user chooses a target by looking at it directly. Because the fundamental frequency of the steady-state visual evoked potential (SSVEP) is equal to the flickering frequency of the target, the correct target can be identified by the BCI from frequency domain activity in the visual cortex (Gao *et al*, 2003). This is typical of the example in 2.2.3.

The independent BCI, on the other hand, does not depend in any way on the brain's normal output pathways e.g. a user would concentrate on a particular letter in a matrix of letters of which a row or column would randomly flash one at a time; and the selected letter is found by observing the P300 (or 'oddball') evoked potential when the particular letter lights up (Allison and Pineda, 2003). This would depend on the user's intent, and not on neuro muscular control needed for precise orientation of the eyes.

2.3.2 Neurophysiological Signals used in BCIs

The positioning of electrodes, signal processing techniques and classification algorithms used in BCIs vary considerably according to the parameters of the BCI concerned. These include the type and source of the signal being measured.

The types of EEG signals that have been used to drive BCIs include slow cortical potentials, P300 evoked potentials, and mu and beta rhythms, visual evoked potentials (Wolpaw *et al.*, 2002).

2.3.3 Slow Cortical Potentials

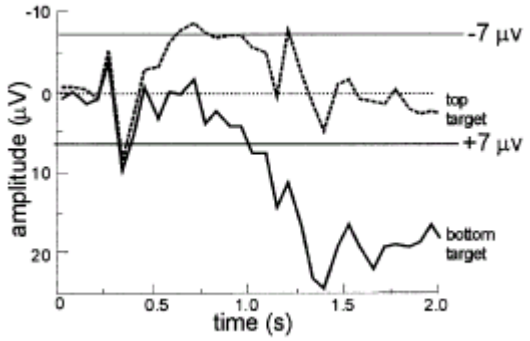

Figure 4. A typical time domain representation of a slow cortical potential. The dotted line is associated with relaxation, while the solid line is associated with cortical activation. (Wolpaw *et al.*, 2002)

Slow cortical potentials (SCPs) occur at very low frequencies of between 0.1 and 2 Hz. Positive SCPs are typically associated with low levels of cortical activation related to a relaxed state in the user, while negative SCPs are produced by movement imagery and other functions involving cortical activation (Birbaumer *et al*, 1999). Figure 4 shows how the difference can be seen in the time domain. It has been shown that people can learn to voluntarily control SCPs (Neumann and Kübler, 2003), and SCP-based BCIs have proven able to supply basic communication ability to people with late-stage Amyotrophic Lateral Sclerosis (ALS) (Kübler *et al.*, 1999, Birbaumer *et al.*, 2003). By varying their SCP voltage level users are able to choose between options presented on a computer screen. Persons with 65-90% accuracy can only write 0.15-3 letters/min, however, which is significantly slower than dependent BCIs. This is due to the very low frequency range of SCPs. On the other hand, this method has proven very useful to people who cannot use conventional augmentative communication technologies.

2.3.4 P300 Evoked Potentials

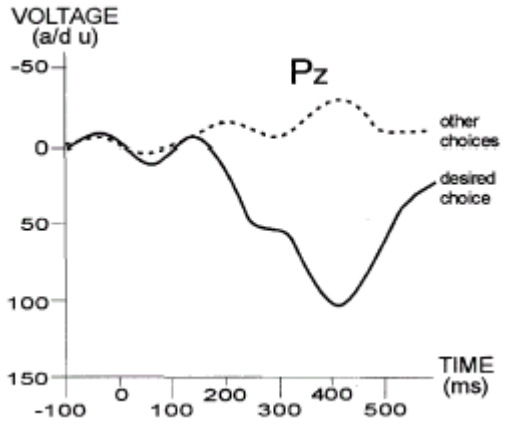

Figure 5. The P300 response is associated with an amplitude increase approximately 300 ms after a stimulus, as seen here in the time domain. (Wolpaw *et al.*, 2002)

A P300 evoked potential (otherwise known as an 'oddball' response) is produced when one observes an infrequently occurring target event. It typically manifests as a positive peak at about 300 ms after a stimulus (as seen in Figure 5), and is measured over most of the parietal cortex (i.e. it has a low spatial frequency) (Niedermeyer and Da Silva, 2004; Guger *et al.*, 2009). Generally P300-based BCIs use a matrix of symbols on a computer screen of which each symbol could be a letter, number, or icon of some sort (Allison and Pineda, 2003). At regular intervals a row or column illuminates randomly on the screen whereupon the user makes his selection by counting how many times his chosen target element has flashed. Every time the element flashes, a P300 is produced. This gives the BCI a clue as to the row or column of the selected element. Analyses using a variety of different processing algorithms suggest that current P300-based BCIs could yield a communication rate of 5 letters/min, and that considerable further improvement should be possible (Piccione *et al*, 2006). Another P300 paradigm involves choosing flashing targets in a virtual reality apartment (Bayliss, 2003), thereby empowering the user to toggle activity of such day-to-day items as a T.V., HiFi system or desk lamp. A limiting factor in the implementation of a P300 BCI is that training is required for every user as introduced in section 2.3.1.

2.3.5 Mu and Beta Rhythms

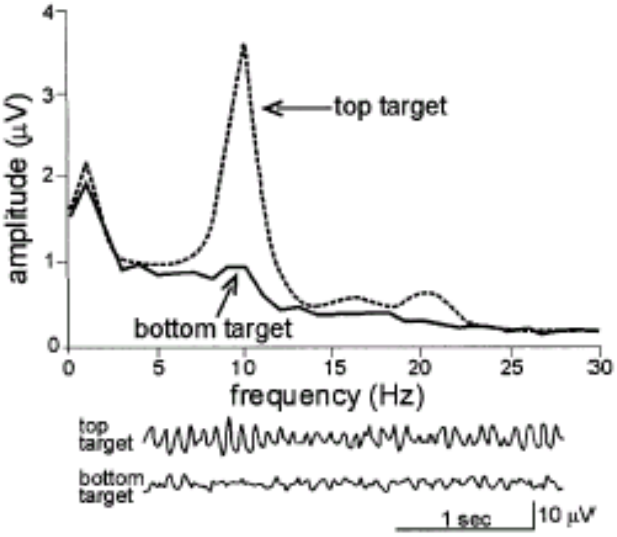

Figure 6. In the frequency domain a peak in the mu range of frequencies is indicative of movement imagery over the motor cortex. (Wolpaw *et al.*, 2002)

Because the amplitudes of Mu and Beta rhythms have been proven to change with movement imagery, they are another choice for direct brain communication. The mu ('mu' stands for 'motor') rhythm occurs in the 8 to 13 Hz band and as such is an alpha rhythm found over the sensorimotor cortex, but related only to movement (Niedermeyer and Da Silva, 2004).

Figure 6 illustrates a mu-rhythm peak in the frequency and time domains. The beta rhythm is found from 14 to 30 Hz and also shows changes related to movement (Wolpaw *et al.*, 2002). The combined frequencies therefore cover a band from 8 to 30 Hz as touched on in section 2.2.1. The areas over which their amplitudes change with movement imagery are directly related to the part of the body which is being imagined to move (see Figure 7).

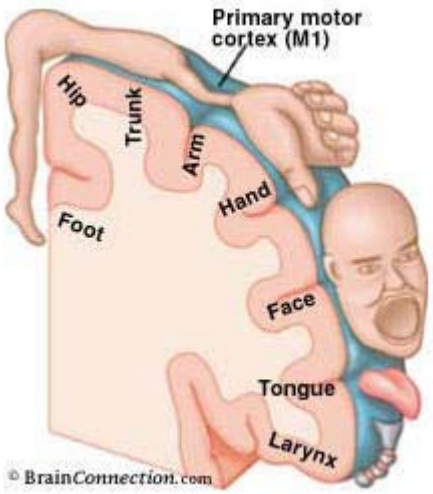

Figure 7. A sagital view of the cortex with an Homunculus indicating areas of the motor cortex relating to movement (Poulin, 2008)

The neurophysiological processes involved in planning movement have been shown to be very similar to those of movement imagery (Pfurtscheller and Neuper, 1997). In particular, both tasks activate the supplementary motor area and premotor cortex (Dechent *et al.*, 2004). In a state of relaxation, the rhythms in the sensorimotor cortex are synchronized, and as such have high amplitude. With the onset of motor imagery (as with preparation for movement) neurons in the cortex become independently activated and the general effect is a resynchronization of the rhythms, known as event-related desynchronizaton (ERD) (Pfurtscheller and Neuper, 1997). The result is an attenuation of mu and beta rhythm amplitudes particularly over the area of the cortex related to the contemplated movement. Even within these frequency bands different behavior is noticeable which can be utilized for more effective classification of mental processes. For example, Pfurtscheller *et al* (2000) found that the 8-10 Hz range showed a non-specific ERD pattern with movement, while the 10-12 Hz band had specific patterns depending on the movement type. Neuper and Pfurtscheller (2001) also found that peak beta oscillations corresponding to foot or hand movement occurred at different frequencies. For the reason of this range of frequencies, this type of BCI also requires training for optimal results.

2.3.6 Visual Evoked Potentials

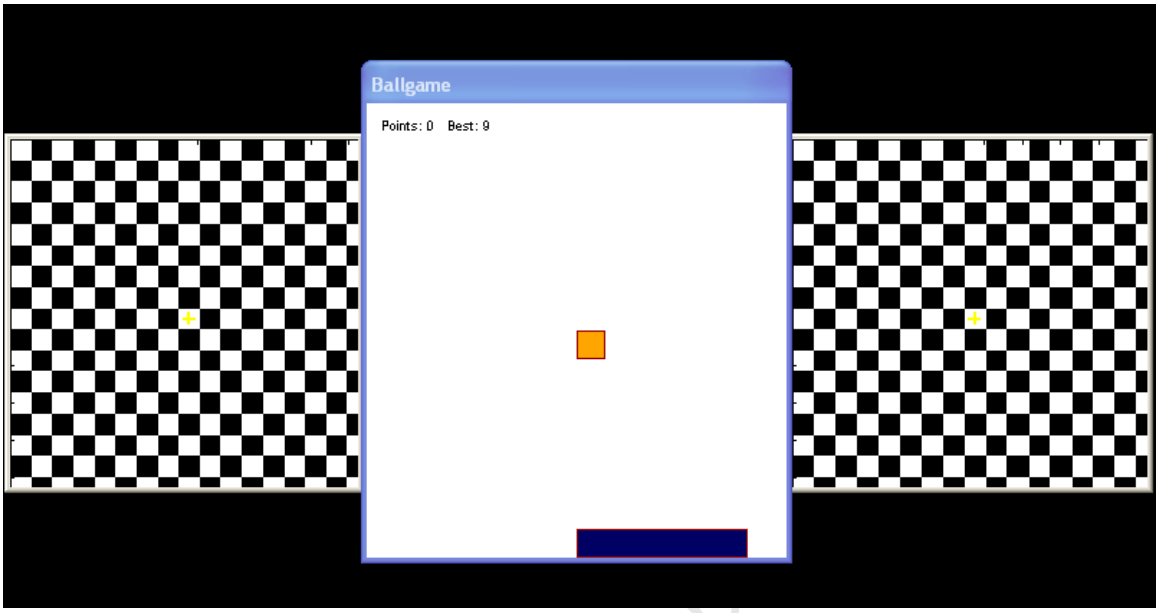

Figure 8. Reversing checkerboards of different frequencies allow a BCI user to move the bar on the bottom of the screen left and right to prevent a bouncing orange ball from falling through the bottom of the window. This setup was developed by the author and was played by visitors to the 2004 Department of Science and Technology Exhibition in Sandton, Johannesburg.

Visual evoked potentials (VEPs) are EEG signals in the visual cortex that are induced by visual stimuli e.g. flashing LEDs or reversing checkerboards on a computer monitor. Figure 8 is an example of a SSVEP BCI with 2 checkerboard stimuli to play a game.

VEP signals used in BCI interfaces are broadly divided into two types: VEPs and SSVEPs (Morgan et al., 1996). VEPs occur at a repetition frequency of less than 2 Hz and as such there is an inactive period between 2 successive stimulations while SSVEPs are a periodic response at frequencies of 6Hz and above (Gao *et al*, 2002).

SSVEPs have been preferred over VEPs in BCIs due the latter's relatively slow repetition rate, although their waveform is the underlying repeated waveform of SSVEPs. SSVEPs are modulated in a similar manner to transient VEPs through visual-spatial selective attention (Muller et al., 1998). The amplitude and phase of the SSVEP are highly sensitive to visual stimulus parameters such as temporal frequency, contrast or modulation depth, and spatial frequency (Regan, 1989).

VEPs have been used successfully to drive BCIs. Sutter (1992) used the VEPs produced from the illumination of a chosen element in a matrix of symbols on a computer monitor as the signal feature to drive his BCI. Using such a system, volunteers operated a word processing program at 10-12 words/min. Another method used several buttons flashing at different rates on a computer screen (Middendorf *et al*, 2000; Gao *et al.*, 2003). When the user looks at a flashing button the BCI system determines the frequency of the photic driving response over the visual cortex (or SSVEP) which would correspond to the chosen button.

Most VEP BCIs are dependent on eye movement. Although such BCIs are capable of great speed and accuracy, this dependence on normal neuromuscular channels has led many researchers to explore the complementing field of independent BCIs (Wolpaw *et al.*, 2002). That said, many people in a locked-in state still have some eye movement, and there are also indications that VEP-based systems may have success as independent BCIs. The related research is covered in some depth in section 3.1.4.

Due to the promise of reported speed and accuracy of SSVEP BCIs and the fact that training is generally not required, it was decided to focus the investigation in this direction.

3 Neurophysiology of the Human Visual System

In order to have a better understanding of SSVEPs measured and manipulated by a BCI it is necessary to investigate the source and generation of the signals. In this case it entails the neurophysiology of visual processing.

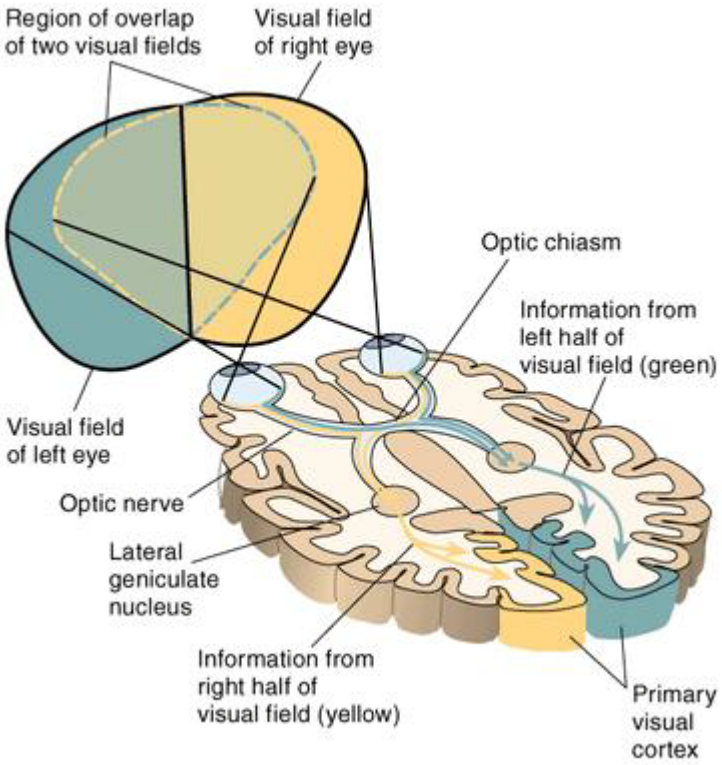

Figure 9. High level axial overview of the human visual system (Kandel *et al*, 2000)

The visual system is the most complex of the sensory systems, with the optic nerve containing an excess of a million fibres. The optic disc, also known as the blind spot is the site where the optic nerve receives the visual information from the external environment. The optic nerves form the optic tract and project to three subcortical areas. Only one of these is suggested to process the visual information that eventually leads to visual perception of the external environment, the lateral geniculate nucleus. The remaining two pretectoral areas that receive neural innervations from the optic nerves relay retinal information for papillary reflexes and eye saccades (Kandel *et al*, 2000).

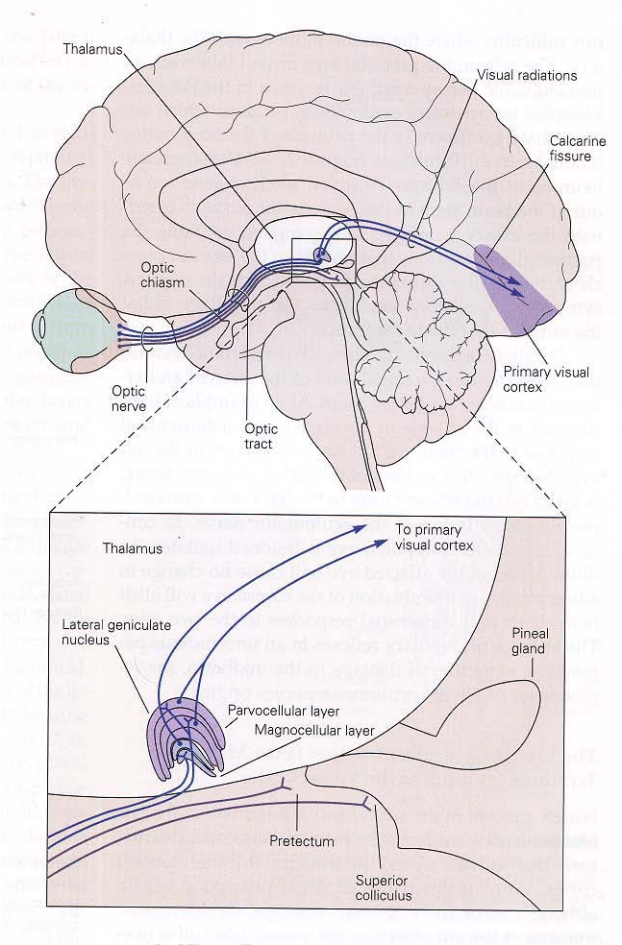

Figure 10. Transverse view of the human visual system with particular attention to the layers of the lateral geniculate nucleus (Kandel *et al*, 2000)

The fovea and nearby area of the retina use about half of the neural mass of the lateral geniculate nucleus while the other represents the rest of the retina. It is separated into 6 layers of which the ventral 2 are known as the magnocellular layers and the dorsal 4 the parvocellular layers (see figure 10). The magnocellular layers receive information from the relatively large M ganglion cells in the retina which respond optimally to high temporal frequency and low spatial frequency. The retinal P ganglion cells are small and numerous and relay information to the parvocellular layers about colour and form. The parvocellular and magnocellular layers also project to separate layers of the primary visual cortex. This anatomical segregation has been described as 2 parallel pathways, referred to as the M and P pathways. Table 1 illustrates their characteristics in terms of Stimuli response. A point to note is that only 10 to 20% of the presynaptic connections in the lateral geniculate nucleus come from the retina. The rest come from other regions and their functions are largely unclear.

	Sensitivity	
Stimulus Feature	**M Cells**	**P Cells**
Colour Contrast	No	Yes
Luminance Contrast	Higher	Lower
Spatial Frequency	Lower	Higher
Temporal Frequency	Higher	Lower

Table 1. Difference in sensitivity of M and P cells to stimulus features (Kandel *et al*, 2000)

The primary visual cortex is approximately 2mm thick and is found on the medial surface of the cerebral hemisphere at the posterior pole. Different areas are devoted to specific parts of the visual field as shown in figure 11. Laterally, it can be divided into 6 layers and further sub layers, 2 of which are where the P and M pathways terminate separately. Neurons in the primary visual cortex create interlayer connections and also outputs to the extrastriate visual cortex areas, the superior colliculus, the pons, the pulvinar, the lateral geniculate nucleus, and the claustrum.

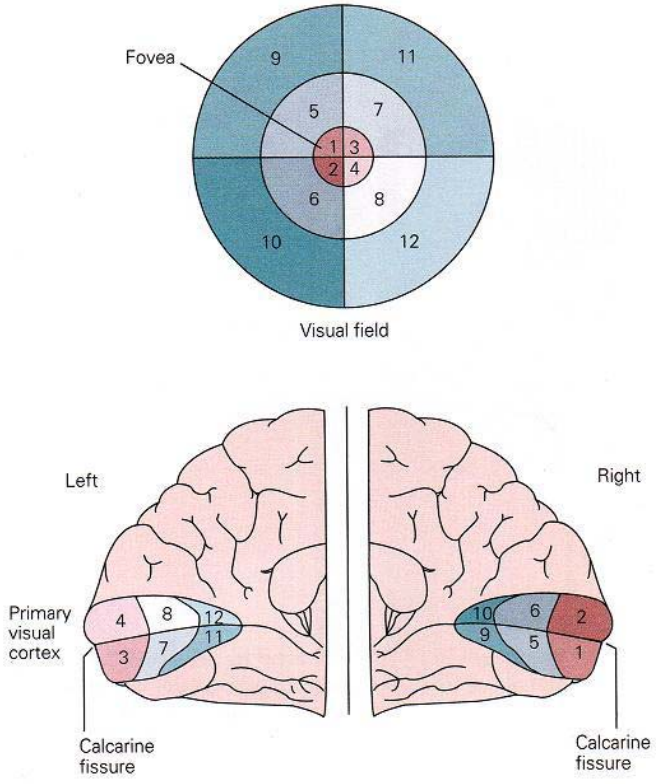

Figure 11. Different areas in the primary visual cortex process information from different parts of the visual field (Kandel *et al*, 2000).

Contrary to the fact that small spots of light excite the cells in the retina and LGN, it has been found that "simple" and correspondingly "complex" cells in the primary visual cortex respond best to linear visual stimuli such as a line or a rectangle. This property allows us to identify edges, thereby enabling recognition of objects. The pyramidal pattern of inputs throughout the visual pathway suggests that every complex cell receives the output of a number of simple cells, each of which receives the output of numerous geniculate cells, each of which receives numerous inputs from retinal ganglion cells.

In the V4 region neurons have been found to have different discharge rates for different shapes of stimuli. Figure 12 illustrates this.

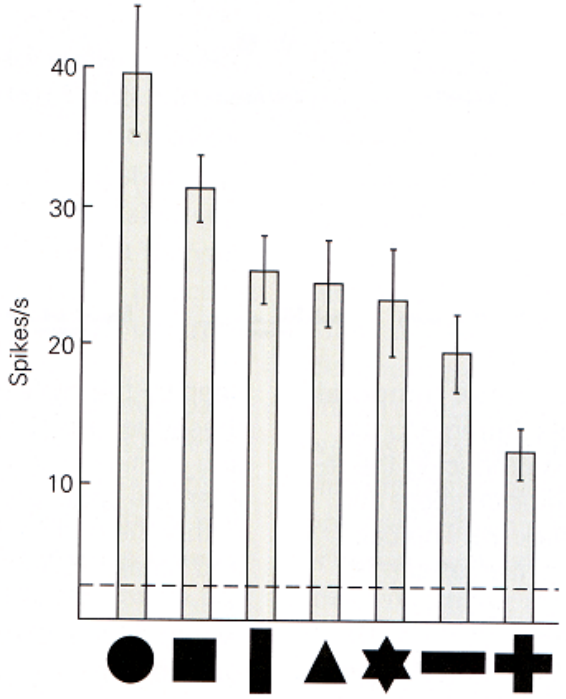

Figure 12. Neurons in V4 have optimal discharge rates for circular stimuli, and vertical stimuli have a higher rate than horizontal (Kandel *et al*, 2000).

While cells in the primary visual cortex respond to the motion of elements of a pattern, PET studies suggest that in humans another area devoted to motion processing is found at the junction of the temporal, parietal and occipital cortices. In the related part of the monkey brain, it has been found that cells respond to motion of a patterned stimulus, like moving bars of light, by detecting contrasts in

luminance. As can be seen in figure 13, this area is in the region of electrodes PO7 and PO8. The difference to the response of cells in the primary visual cortex is that in this case, a motion stimulus at any position in a wide range of the visual field provokes a response. In the primary visual cortex, only a specifically positioned edge will induce neuronal excitement.

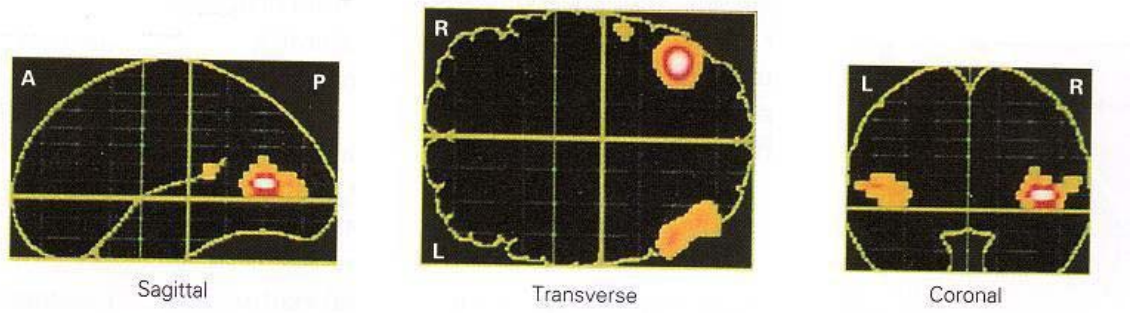

Figure 13. PET images indicate activity around electrodes PO_7 and PO_8 related to moving stimuli and therefore motion processing (Kandel *et al*, 2000).

4 SSVEP Literature Review

4.1 Stimulus Parameters

To generate SSVEPs which are optimal to monitor, we need to understand how to optimize the parameters of the stimuli which generate the signals in the cortex. Much has been researched in this area, many researchers looking at specific parameters of the stimuli, while some like Beverina *et al* (2003) and Regan (1989) undertook numerous studies for a more comprehensive approach. Beverina, for example, performed experiments to achieve, as stated, optimal use of electrode placement, light intensity, colour, shape, dimension and flickering frequency to increase the amplitude of SSVEP signals responding to the stimulus (the methodologies of these tests were however not provided and only limited results were reported pertaining mainly to frequency and electrode position).

What follows is a description of some of the stimulus parameters involved in SSVEP BCIs and a review of literature concerned with exploration thereof. Due to the large number of variations between experimental setups in different studies it is difficult to directly compare results such as bit rate of information transfer or correct classification accuracies. Parameters like these include room luminance, BCI hardware platform, experimental protocol, feature extraction and classification methods, number of electrodes, and many more. Direct comparisons are also difficult due to the fact that different measures are used to quantify results, e.g. signal to noise ratio, information transfer rate and others.

4.1.1 Temporal Frequency

According to Regan(1989) the VEP waveform produced by visual stimulation with flickering unpatterned light can be fairly well understood in terms of three functional subsystems working in parallel: a high-frequency subsystem (30-60 Hz), a medium-frequency subsystem (14-30 Hz), and a low-frequency subsystem (6-14Hz). See figure 14. Wang *et al*, 2006 achieved similar results when testing a SSVEP BCI.

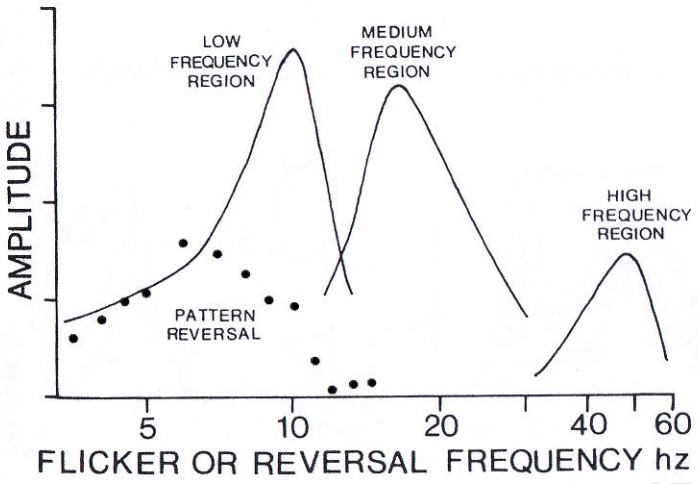

Figure 14. Amplitude of SSVEP response is separated into 3 subsystems (Regan, 1989)

Gao (2003) investigated only the low frequency band for the 4 following reasons as stated:

- The amplitude of the evoked potential in the medium and high frequency bands is lower than that of the low frequency band.
- Responses in the medium and high frequency bands may be induced by stimulations at second harmonics or subharmonics which violate the unique frequency relation between excitation and response.
- According to physiological research, response in the low-frequency band may become saturated more easily. This characteristic makes the response more robust when the surrounding brightness varies.
- Low- and high-frequency responses have different topographical distribution. The former has a wide distribution over the head, whereas the latter is comparatively restricted in topography. Thus, it is easier to place the electrode on the scalp when the low-frequency band is used (section 4.4 elaborates more on electrode placement).

The optimal range (for higher selection accuracy and shorter response time) in the low frequency band was found to be between 8 and12 Hz, but the 10 to 12 Hz range was recommended to exclude instantaneous alpha band interference found in the 8 to 10 Hz range in the subjects.

Gao also found that the minimal differential frequency resolution for a SSVEP was 0.195 Hz - determined empirically from the range of frequencies used (6 to 15 Hz) and the number of separately identifiable light stimuli (48 flashing LEDs).

Noise introduced by computer monitor refresh rates is discussed in literature (Wang *et al,* 2008; Zhu *et al*, 2010). It has been found that the noise is reduced if the stimulation frequencies are chosen to be factors of the refresh rate of the computer monitor producing the stimulus (see section 6.1.1.). Beverina *et al* (2003) chose frequencies of 6 and 10 Hz for stimulation since they and their harmonics have minimal interference. Although the refresh rate of the monitor was not mentioned in this paper, it is suspected to have been either 60 or 120 Hz since the selected frequencies are factors thereof.

Many other studies have used different stimulation frequencies to those already mentioned. Reasons for concentrating on particular frequency bands are often due to their suitability for feature extraction methods and classification methods employed. For instance, Gao recommended excluding 8 to 10 Hz frequencies because of unrelated Alpha noise (found in their subjects), but other researchers have used these frequencies effectively, with some compensating for the noise with feature extraction strategies (Allison *et al*, 2008; Nielsen *et al*, 2006).

Harmonics of SSVEP frequencies have been used with some success to better extract and translate intentions of the user of a BCI. A harmonic is a component frequency that occurs at integer multiples of the fundamental frequency, which in this case is the stimulation frequency. Muller-Putz *et al* (2005) found that the use of 3 harmonics with their classification techniques yielded a significantly higher classification accuracy. Harmonics were also used by Nielsen *et al* (2006) to aid in classification between 9 possible choices presented to a subject.

In addition to the use of harmonics, overlapping stimuli with different frequencies have been used to elicit responses with the frequencies and additions of the frequencies to aid in classification (Mukesh *et al,* 2006).

Subharmonics can also be present in a SSVEP power spectrum. Mukesh *et al* (2006) attributed this to raspers observed at half the stimulation frequency on the stimulus present on a CRT. A rasper is an

average colour that occurs between colours when a screen is repainted and was observed during the experiments conducted by the author.

4.1.2 Colour and luminance

In terms of colour, the human eye is less sensitive to light in the red and blue parts of the light spectrum, while optimally sensitive in the green area at 510nm (at 1700 Lumens/m2 of pupil area/ Watt) and 555nm (at 683 lumens/m2 of pupil area/Watt) wavelengths for low light levels (below about 0.003 Candela/m2) and high light levels (above about 0.003 Candela/m2) respectively (Regan, 1989)

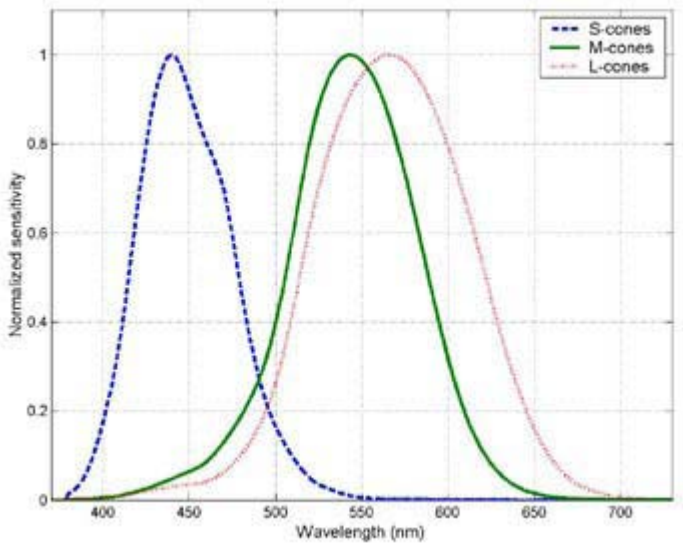

Figure 15. Graphical representation of the relative sensitivity of the human eye to different colours (nikondigital, 2010).

Arakawa *et al* (1999) compared chromatic (red-green gratings) and achromatic (white-black gratings) with respect to the SSVEP response across spatial frequencies. They found that the amplitude of chromatic induced SSVEPs exhibited a decrease in the 2nd harmonic at higher spatial frequencies while the 4th harmonic amplitude showed no dependence on spatial frequency. The results of Arakawa *et al* (1999) also indicate that the mean of the 2nd harmonic SSVEP amplitude for the chromatic stimulus was greater than that for the achromatic stimulus, but was the opposite for the 4th harmonic response. This study is covered also in section 4.1.4 under spatial frequency.

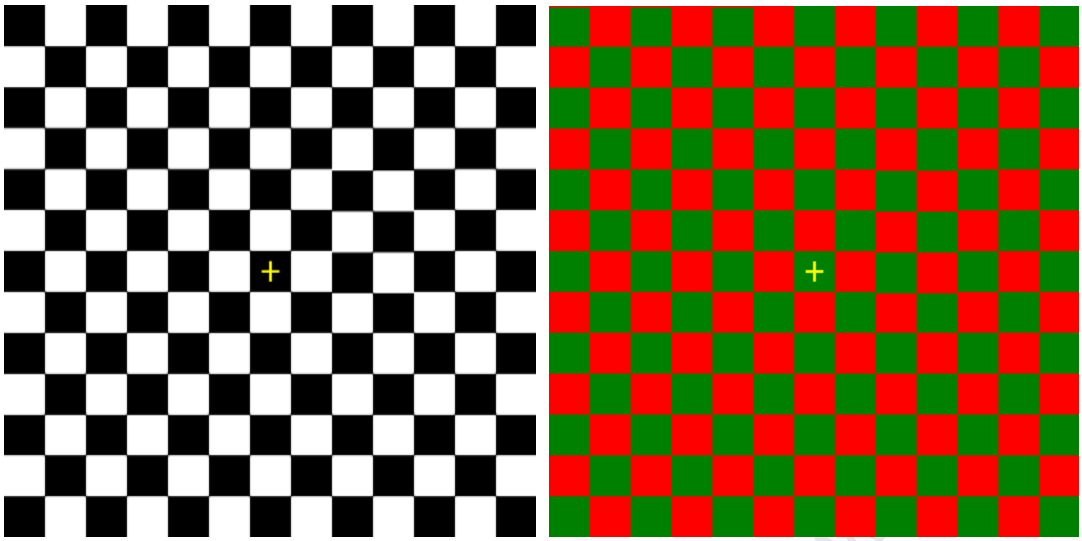

Figure 16. Black and white, and red and green checkerboards have different effects on harmonics of stimulation frequencies

Colours have also been used to produce multiple-frequency SSVEPs which allow for a greater number of peaks in the f-domain for classification (Cheng *et al*, 2002). To achieve this, different stimulation frequencies of different colours are overlapped to produce a multi-colour irregular-seeming stimulus which induces SSVEP signals at sums and differences of these frequencies. The frequencies were combined by using different colours to signify dual high, dual low and single highs.

It has also been suggested by Wang *et al* (2008) that different colours can be used to enable a user to choose overlapping stimuli of different frequencies by focusing on a specific colour which would be flickering at a particular frequency.

4.1.3 Size of stimuli

Because the physiological stimulation produced in the eye depends on the area of the retina that is illuminated, the size of the pupil largely determines the retinal illuminance. It makes sense therefore, that between certain light thresholds (causing constricted or dilated pupils), the behavior of the retinal illuminance over the light spectrum can be fairly well defined (Regan, 1989). For the case of this study it was thus decided to perform experiments in a darkened environment. See the experimental setup in section 6.1.

To describe it more mathematically, a luminous surface area S m^2 and luminance B cd/m^2 is observed by an eye with an entrance pupil of area A m^2 situated u m from the surface. By definition the luminous flux per unit solid angle is equal to BA lumens/steridian. Therefore the total luminous flux entering the eye is equal to BSA/u^2 lumens. This would have a bearing on the size of the stimulus being presented to a subject in a SSVEP experiment (Regan, 1989).

4.1.4 Spatial Frequencies

Spatial frequency is a measure of how often an arrangement repeats over distance. In the case of SSVEP BCI stimuli an example would be the size checks in a reversing checkerboard (See figure 17). This is illustrated in figure 17.

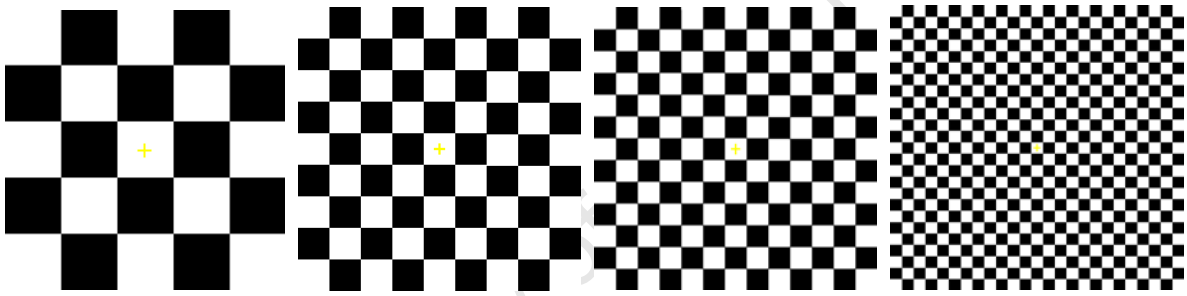

Figure 17. 4 checkerboards with increasing spatial frequency from left to right.

In literature, spatial frequency is usually referred to in terms of cycles per degree (cpd). This indicates how many repetitions of an arrangement there are for a one degree angle of view. In SSVEP experiments this is dependent on the distance of the subjects' eyes from the stimulus. Figure 18 illustrates the concept.

As has already been touched upon, Arakawa et al (1999) investigated the effect of spatial frequency of chromatic or achromatic stimuli on SSVEPs. They investigated the assertion that visual information is processed mainly by the two parallel visual pathways, the P and M pathways discussed in chapter 3.

Because of reports that the 2^{nd} and 4^{th} harmonics are differently affected by spatial frequency, aging, and binocular stimulation, it was hypothesized that they were generated by functionally and anatomically distinct neuronal populations.

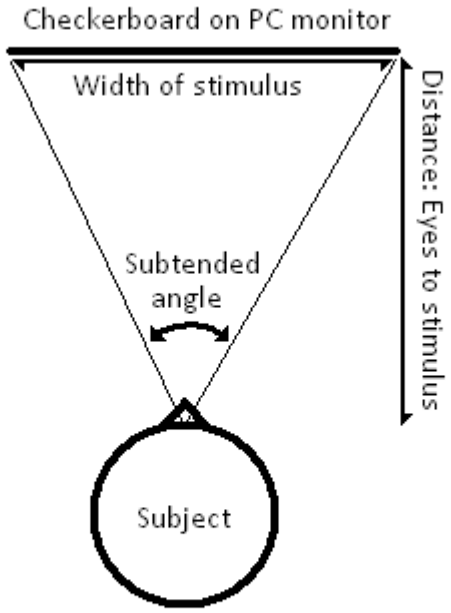

$$\text{Subtended angle} = 2\tan^{-1}\left(\frac{\text{Width of stimulus}}{2 \text{ X Distance: Eyes to stimulus}}\right)$$

Figure 18. The angle subtended by a stimulus is computed from the size of the stimulus and the subject's distance from the stimulus.

In the study, 13 subjects were required to look at a 11.9X7.8 degree screen where chromatic and achromatic stimuli were presented at 9 spatial frequencies from 0,5 to 8 cycles/degree (cpd). An electrode placed at O_Z was referenced to F_Z, and the data was 0.5-120Hz band-passed with a sample rate of 500Hz.

It was found that at lower spatial frequencies the mean 2nd harmonic amplitudes of chromatic SSVEPs were significantly larger than those of achromatic SSVEPs. The chromatic SSVEPs showed a low-pass characteristic dropping off at about 4cpd at the 2nd harmonic while the chromatic showed a bandpass characteristic peaking at about 4 cpd. The mean amplitude of achromatic SSVEPs at the 4th harmonic were smaller in magnitude and less varied across the range of spatial frequencies than that of chromatic SSVEPs which exhibited a high-pass characteristic with the increase starting at about 1,3cpd (with a slight drop off at 8cpd).

4.1.5 Direct and Covert Attention

In order to realize an independent SSVEP BCI, users would need to select from a choice of stimuli without moving their eyes. In this case, covert attention should be focused on a stimulus, meaning that the brain would focus on information coming from a certain part of the peripheral vision. Covert attention to stimuli will induce related SSVEPs which can be measured, albeit with low amplitudes. The relationship of spatial attention and related SSVEPs has been the subject of a few studies.

According to Regan (1989), SSVEP amplitude modulations can be attributed to a sensory gain mechanism that acts at the level of the extrastriate visual cortex and amplifies visual inputs within the spotlight of attention.

Hillyard *et al* (1997) and Muller *et al* (1998) found that SSVEP amplitudes were of greater magnitude when covert attention was focused on the 8 to 12 Hz and 20 to 28 Hz ranges. These correspond to the 'low' and 'medium' SSVEP frequency ranges described by Regan (1989). See figure 14.

In the Muller study, 25 subjects were presented with 2 stimuli 10 degrees apart that comprised 5 vertical LEDs at a length of 3.45 deg by width of 0.5 deg, and flickering at 20.8 and 27.8 Hz on the left and right respectively. 26 electrodes over the whole head were monitored, as well as electrodes for EOG. The signals were band-passed at 0.3-100Hz and digitized at 250Hz. When subjects were covertly attending one of the stimuli the average SSVEP amplitudes at that frequency increased while the SSVEP response from the unattended stimulus showed little change from the amplitude when the subjects were attending a point between the stimuli.

In a similar experiment, Kelly *et al* (2005) investigated the effectiveness of a SSVEP BCI when no ocular motor control was used. 11 subjects participated in the study and were seated 60 cm from a CRT monitor with 2 stimuli of a single check flashing at 10 and 12 Hz of size 3.6X4.7 degrees separated by 5.8 degrees. By comparing the power spectrums found when a subject covertly attended a stimulus to the baseline power spectrum recorded at the beginning of the trial sessions, they were able to achieve limited success in that 5 of 11 subjects managed at least some satisfactory results.

In an interesting study by Muller and Hubner (2002) two different sizes of capital letters were superimposed on each other and flashed at different rates. Letters were 11.3 X 5.1 deg and 1.72 X 1.15 degree in size and were flashing at 7Hz and 11.67 Hz respectively and vice versa. Electrodes were placed over the temporal, parietal and occipital lobes according to the 10-20 system. SSVEP amplitudes were found to be significantly enhanced for the attended letter stream as compared to that of the ignored stream. This indicated that the attentional focus can exclude some objects in its path.

4.1.6 Type of stimulus: Checkerboard vs flicker

Wu *et al* (2008) undertook a study of stimuli by comparing LED flicker, CRT reversing checkerboards, and LCD reversing checkerboards. They found that LED flicker elicited the greatest amplitude response for fundamental frequency and harmonics while CRT and LCD were fairly similar in this aspect. The CRT was seen to be affected by the refresh rate while the LCD did not, and the LCD also showed many low frequency components which were not present in the other stimuli.

Lyskov *et al* (1998) also found that subjects exhibited SSVEPs corresponding to computer monitor flicker, in this case 60 Hz and 120 Hz.

Lalor *et al* (2005) on visual inspection found that a checkerboard stimulus elicited more pronounced SSVEPs than a flicker stimulus for the same frequency.

4.2 Visual feedback

Beverina *et al* (2003) added a 'biofeedback bar' next to the stimulus by which the subject could observe their measured response. It was found that this helped to adapt the SSVEP response to what was required by the classification algorithm, with a range of 9 to 35% increase. Correct classification was achieved 95.71 percent of the time on average across all subjects but the bit rate was low (10 in 97.16 seconds) because the thresholds were set high to avoid false negatives. Beverina concluded that the bit rate increased according to how much the subject was concentrated on the task, and suggested that the study of interfaces and stimulation strategies are therefore critical.

4.3 Adaptation Characteristics

Heinrich and Bach (2001) investigated adaptation to pattern reversal SSVEPs as well as inter-subject variability. In their study, O_Z was used referenced to the earlobes of 19 subjects, band passed from 1-100Hz and sampled at 500Hz. Check size was 1.3 degrees and frequency was 8.3Hz.

Subjects were exposed to 3 different stimulation protocols: continuous stimulation for 1 minute; 2 sec bursts of stimulation interspersed by 2 sec isoluminant grey background for 1 minute; and 2 sec bursts of stimulation interspersed by 12 sec isoluminant grey background for 1 minute. It was found on average that there was an initial stimulation period (increase in amplitude of SSVEP) for an average of 8.2 +- 6.3s whereafter there was an exponential decline due to adaptation for the continuous stimulation. The 2nd protocol mirrored this trend but showed a slightly slower onset of the adaptation period, lower maximum amplitude, and less drop off due to adaptation. The 3rd had lower amplitude with no noticeable initial stimulation, and what was interpreted as a linear drop off which was nearly horizontal by comparison to the previous two protocols' results. The smaller amplitude could be attributed to the long periods between stimulation which negated the development of an initial stimulation period.

It was noted that the 4th harmonic time course did not mimic that of the 2nd harmonic which suggests that different processes are involved in the generation of this element.

The initial increase in amplitude was mirrored by experiments of single cell activity and there has been speculation that the delay is caused by tonic inhibition between neighbouring spatial frequency channels.

Heinrich and Bach (2003) found that SS motion VEPs did not suffer from adaptation. These are different to the checkerboard SSVEP in that the stimuli change over time and as such prevent adaptation. They also found large differences between amplitudes of SSVEPs of subjects, all exposed to a stimulus of 13Hz

In order to cancel adaptation effects Gao *et al* (2003) employed a protocol in which a short period was allowed for the subject to adapt to flickering stimulation.

Beverina *et al* (2003) reported a decrease in signal amplitude after about 7 trials (see figure 19), and attributed this to fatigue due to subject reports of tiring and difficulty to concentrate. Each trial had a 20 second stimulus, but the rest period was not stipulated.

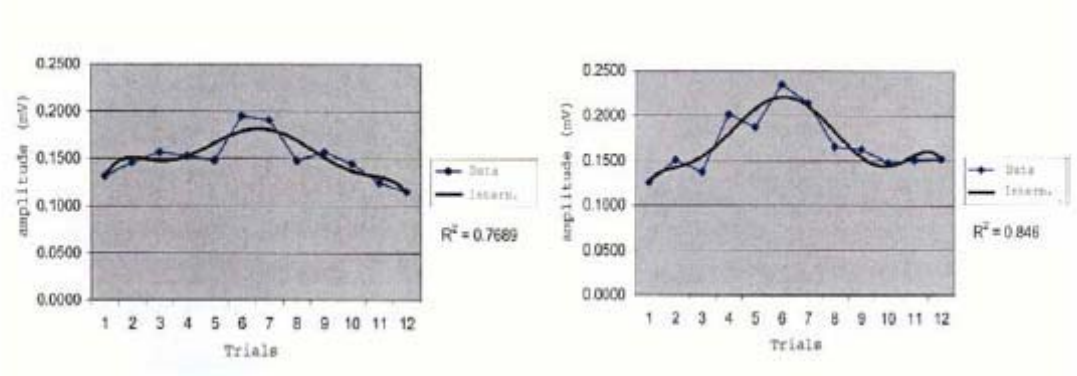

Figure 19. Subjects presented with 20 second duration trials for both 6 (left) and 10 Hz (right) stimuli experienced an initial stimulation period peaking at 6-7 trials whereafter there was an amplitude decline (Beverina *et al*, 2003).

4.4 Electrode Placement

The International Society for the Clinical Electrophysiology of Vision (ISCEV) specifies that to record the VEP an electrode setup of O_Z and F_Z be employed for the active and reference electrodes respectively. Mackay *et al* contends that a greater SNR can be achieved by better electrode placement. They suggest that the further apart the reference and active electrodes, the less coherent the measured noise will be, resulting in little or no noise cancellation. Although the signal amplitude is reduced in bipolar recording, which uses a reference site much closer to the active site, the cancellation of coherent noise results in a higher SNR (Wang and Zheng, 2008).

With a view to improving SNR by electrode placement, MacKay *et al* (2003) set out to explore the benefits of using 3 active electrodes in various 1D Laplacian analysis layouts centred on O_Z with a common reference at F_Z. This would take advantage of the spatial frequency of the signal to achieve a higher SNR.

It was shown that using electrode sites 15% and 20% of half the head circumference lateral to Oz, the Laplacian layout proved to detect VEPs significantly faster for checkerboards consisting of 3' checks, but there was no improvement for larger checks for any spatial distribution of electrodes. In fact, on average for all spatial distributions and stimuli, the Laplacian setup took on average longer to detect a VEP. The relationship between SNR and the BCI detection speed is that the speed of the BCI was faster when provided with a higher SNR in the SSVEP signal.

The absence of the simultaneous laterally measured striate response to the small stimuli would mean minimal signal cancellation, therefore lending itself to increased SNR. To explain this, it is suggested that signal amplitude drops off at about 15% head circumference when moving laterally (with peak at O_Z), while the noise coherence drops off between 20 and 25 % of half head circumference.

According to Beverina *et al* (2003), checkerboard with checks of 11' on a 12 degree field were found to elicit travelling waves with rapid attenuation from occipital region to P_Z with most subjects while the flicker stimulus elicited standing waves of greater magnitude which had a phase reversal at P_Z but maintained amplitude over the prefrontal area. It was found after testing 5 subjects that the occipital electrodes measured higher SSVEP amplitudes, particularly PO_8 (This electrode has not been found to have significantly higher amplitudes in any other literature however). The second harmonic was found to be of the greatest amplitude of all.

Wu and Yao (2008) set out to quantify different electrode positions' performance by introducing a "stability coefficient". The stability of the power spectrums of SSVEPs at different sites were compared and it was found that SSVEPs over the occipital region were the most stable over time.

4.5 Baseline

Traditionally a baseline is taken when a subject is relaxed with eyes open and not attending a flashing stimulus (Muller-Putz *et al*, 2008; Bakardjian *et al*, 2010; Prueckl and Guger, 2009; Muhl *et al*, 2009).

It was found by Muhl *et al*, 2009, that alpha power was higher before a subject was attending a SSVEP stimulus than during the stimulus attention.

Mulholland and Peper (1971) investigated "alpha blocking" which occurred when a subject was attending to a visual stimulus. They concluded that the attenuation was not due to visual attenuation but to "processes of fixation, lens accommodation, and pursuit tracking".

4.6 Signal to noise ratio

Vialatte *et al* (2010) described the SNR as the "ratio of Fourier power at frequency f and average Fourier power at its n-adjacent frequencies".

Signal to noise ratio (SNR) has been used to indicate efficacy of stimuli and feature extraction procedures (Vialatte *et* al, 2010; Wang *et al*, 2006; Wang *et al*, 2004; Gao *et al*, 2004).

Generally the signal to noise ratio is taken as the amplitude or power of the signal in the frequency domain divided by the average amplitudes or powers over a specific range of frequencies. Gao *et al*, 2004 used a range from 1 Hz less to 1 Hz greater than the signal frequency. Wang *et al*, 2004 used a range from minus to plus 4 Hz of the signal frequency.

4.7 Other Considerations

The SSVEP has been found to have widespread reduced latency when subjects are shown pleasant or unpleasant images. This indicates that the perceived emotional value of the stimulus modulates the response.

5 Objective of Investigation

5.1 Critique of Literature

- A standard practice in much of the literature is to use a baseline measurement of EEG activity to aid in feature extraction. This baseline is obtained when a subject is at rest with no stimulus. The effect of task-related concentration has not been considered in the past when choosing a baseline to eliminate unnecessary noise.
- The comparative effect of PC monitor generated shapes of stimuli on the SSVEP has not been investigated despite there being much information regarding how groups of neurons of the visual cortex respond to straight lines in particular orientations (Kandel *et al*., 2000).

5.2 Aim

The aim of the investigation described in this dissertation is two-fold.

5.2.1 Investigation of an activity baseline to reduce background EEG

To investigate a method potentially enabling a SSVEP-based BCI to improve feature extraction on an ongoing basis. The premise is that in generally accepted practice, a "resting baseline" of EEG activity when a subject is not attending any stimulus is used in order to determine by comparison when a subject is in fact attending a particular stimulus (Kelly *et al,* 2005). It is hypothesized that if an "activity baseline" derived from task-related activity is used for feature extraction it will prove more effective than a resting baseline.

5.2.2 Investigation of the effect of shapes on the SSVEP

To investigate the effects of vertical and horizontal rectangular and striped reversing patterns on the SNR. It is hypothesized that vertical patterns will have a better SNR based on single neuron activity as described by Kandel *et al* (2000). See figure 12.

6 Methodology

6.1 Experimental Setup

A 6 lead modularEEG which was assembled in the lab is to be used for acquisition, amplification and digitizing of the EEG activity. The amplifier has been used by researchers in the past and proven to be comparable to commercially available systems (Mukesh *et al,* 2006). Figure 20 shows the modularEEG.

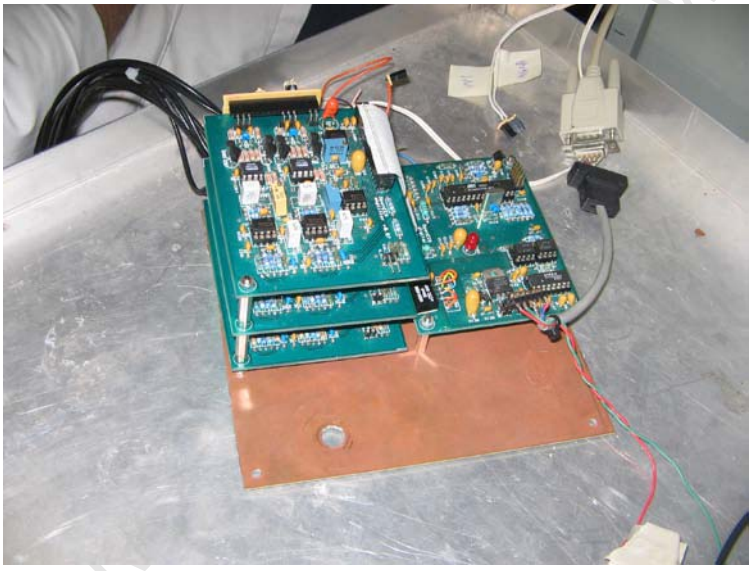

Figure 20. A 6 lead modularEEG comprising 3 analog amplifier boards on the left and 1 digital board on the right.

The electrodes are passive electrodes and were constructed in the lab by the author (see Appendix A). They comprise two different designs because the author developed easier-to-manage electrodes as the study went on. The 6 electrodes were placed at F_Z, O_Z and 2 points lateral to O_Z on both sides at 10% and 20% of the half head circumference from O_Z.

The signals are digitized by the modularEEG at 256Hz and transmitted via RS-232 to a Desktop PC via the serial port. The software used for capturing the data was an open-source program known as Brainbay. All experiments took place in a darkened room (4.1.3) with the subject seated in a chair. See figure 21.

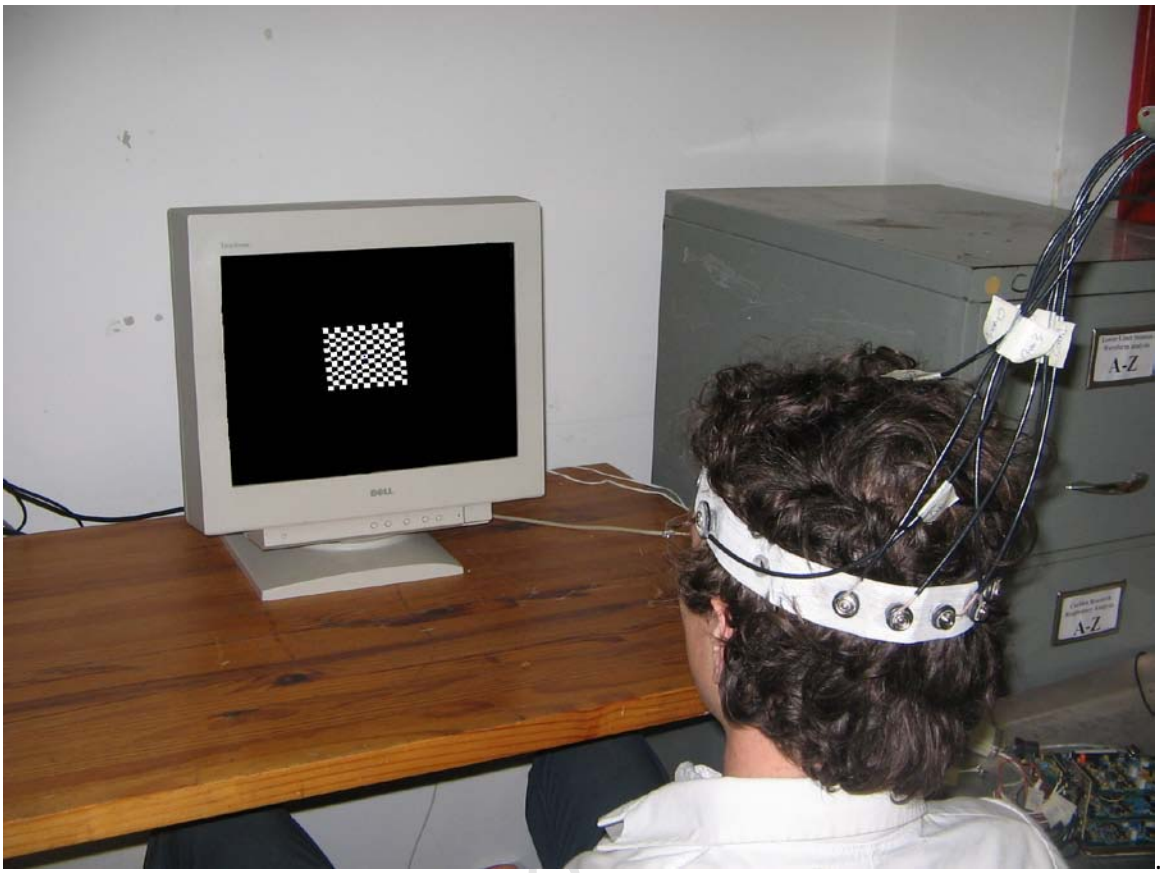

Figure 21. SSVEP experimental setup. A subject attends the stimulus on the computer monitor. EEG electrodes which have been developed in the laboratory by the author are attached to the custom-made elastic electrode band such that the electrodes are at PO7, O1, Oz, O2, and PO8.

6.1.1 Shape of Stimuli Experiment

Ethics approval was obtained for the experiment as indicated by the ethics number 296/2004.

The shapes used for stimuli were checks and vertical and horizontal rectangles and lines all with the same width as shown in figure 21. The subject was placed 52cm from a CRT with refresh rate of 120Hz so that the widths of the stimuli subtend an angle of 1˚. The subject was required to focus on each shape of stimulus for 20 seconds with a 10 second break each time, at a range of frequencies. The frequencies selected were 8, 10, 12, 15 and 20 Hz in that order and the shapes of stimuli were presented in the order from left to right of figure 22.

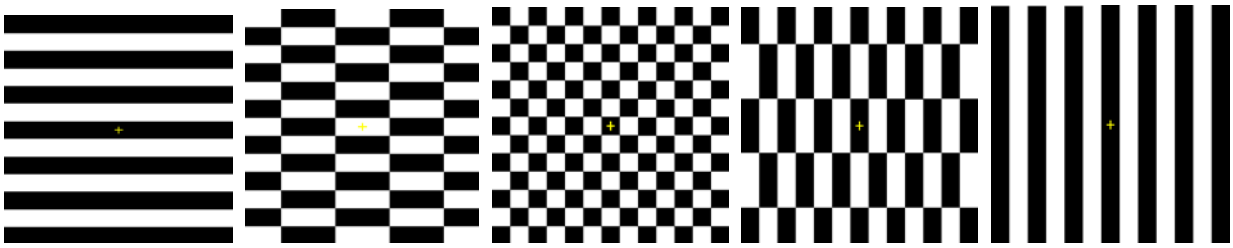

Figure 22. Stimuli presented to subjects are reversing boards with horizontal and vertical lines, horizontal and vertical rectangles, and checks, all of the same width.

The 20 second duration of stimulus was the same as that used by Beverina *et al* (2003) as mentioned in section 4.3. A further benefit of using such a long stimulus was that PC generated stimuli have been reported to freeze (Zhu *et al*, 2010) and a longer stimulation period would allow such an occurrence to be better averaged out (see section 6.2.2.). The rest period of 10 seconds was chosen to be similar to the rest period of Heinrich and Bach (2001) of 12 seconds, where the post initial stimulation was followed by a long period of minimal drop off (almost level amplitude). This would aid in combating adaptation or fatigue in subjects. Although using SS motion VEPs (Heinrich and Bach, 2003) may have reduced the adaptation further, this method has not been extensively researched, and as such to limit any unknown related effects, they were not used.

The stimulation frequencies were chosen to be factors of the refresh rate of the CRT (120 Hz) so as to ensure as little influence from screen refreshing as possible (Wang *et al,* 2008; Zhu *et al*, 2010) (See 4.1.1.).

Since the colour of the stimuli have previously been extensively investigated and black and white reversing stimuli are the most common, they were chosen for this experiment (Zhu *et al*, 2010) (4.1.2.). The size of the stimuli (4.1.3.) and spatial frequency (4.1.4.) were chosen to be the same so that there would not be any influence from these parameters on the SSVEP amplitude.

The electrodes used to capture the EEG were passive Silver/Silver Chloride electrodes made by the author. They were chloridized by passing a current through a 1:50 HCl solution using the silver electrodes on the positive voltage. The electrodes were placed inside small sponges which were soaked in EEG gel and held in place on the subjects' heads by means of an elastic headband. See Appendix A for more information on electrode development.

6.2 Analytical Methodology

MATLAB release 13 was used as a tool to process experimental data extracted from brainbay archive files. More information regarding data structures and MATLAB code is available in Appendix B. The processing is summarized in figure 23.

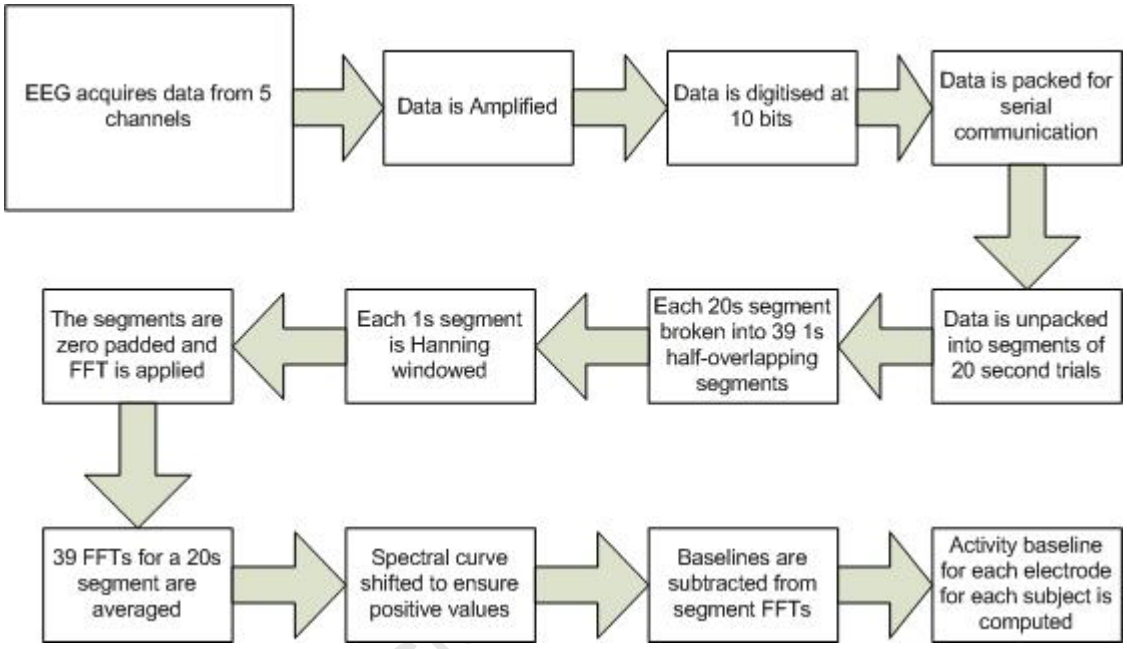

Figure 23. Matlab processing of data is represented in a block diagram.

6.2.1 Unpacking of Data

The data was unpacked into files with arrays of 6 channels by 5120 points of data representing 1/256 seconds per point for the first experiment, and 3072 points of data for experiments 2, 3 and 4. The 6 channels represented the reference at F_Z, O_Z and 2 points lateral to O_Z on both sides at 10% and 20% of the half head circumference from O_Z.

6.2.2 Measure to counteract correct phase change from freezing stimulus

In some cases the reversing stimuli on the PC monitor were seen to hang for a fraction of a second. This type of incident would change the phase of the stimulus and as such affect an overall FFT of that period of testing. As a result it was decided to perform FFTs of every 1 second (256 points) of the data with a

0.5 second overlap and average these over the duration of a particular test. Effectively, any phase changing component of the stimulus would be averaged out and have only a minor effect on the result. For instance, if it was assumed that over a 20 second epoch a monitor freeze occurred twice, there would be 4 out of 39 1 second FFTs affected by the phase change.

6.2.3 The FFT and rendering of Data

Every one second of data was zero-padded by 256 zeroes and a Hanning window was applied. The resulting average spectrum over the test was a 1 by 512 array of data points. Once the average spectrum of each test in each experiment had been obtained, these arrays were placed in a two-dimensional MATLAB cell where subjects were the rows, and tests were represented by columns. This rendering of the data made it possible to easily determine similarities across subjects for individual tests as well as performing normalization of data and subtraction of baselines per subject. Examples of the MATLAB code used can be found in Appendix B.

6.2.4 SNR

The SNR was calculated as the sum of the powers of the stimulus frequency and its 2^{nd} harmonic, divided by the average power from 8 to 30 Hz for all but the 20 Hz stimulus. For this the power at the subharmonic was added to that of the fundamental frequency since the subharmonic was observed to be significant. The wide band was chosen so that it included all stimulation frequencies of interest and the relevant harmonics and subharmonics. All of these frequencies are of interest because ultimately a classifier would need to choose which one of the stimulation frequencies is being attended in a working BCI. If there were to be activity in the wrong frequency band, it would need to be reflected in the author's measure of the SNR.

6.2.5 Calculation of Resting and Activity Baselines

In each experiment the subject was asked to attend a non-reversing checkerboard for 20 seconds in order to obtain an open-eyes baseline, and to close their eyes for 20 seconds to obtain a closed-eyes baseline against which the SSVEP could be measured. The spectra from these baselines were processed in the same way as the SSVEP spectra, namely with 1 second Hanning-windowed half-overlapping FFTs which were normalized as above.

In addition to the non-stimulus baseline, a third “activity baseline” was calculated based on the average spectra for each subject over all experiments. This was done by taking the normalized spectrum for all experiments per subject and averaging them. Examples of the three baselines are shown in figure 24.

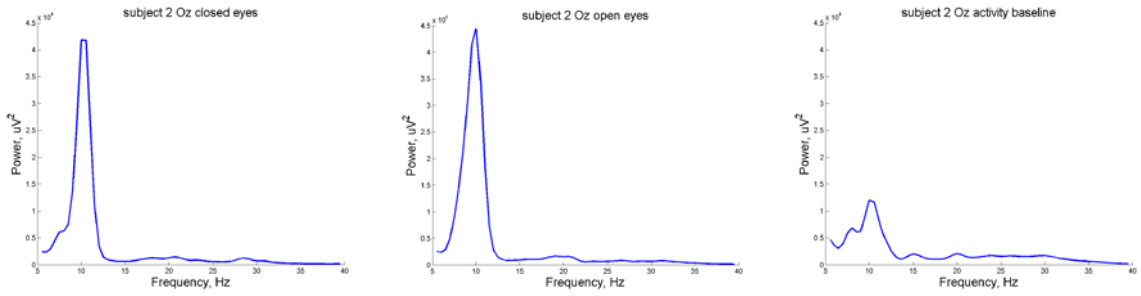

Figure 24. Both the closed-eyes and open-eyes baselines show pronounced alpha activity. The activity baseline has a much reduced alpha while it shows peaks at the stimulation frequencies of 8, 10, 12, 15 and 20 Hz since it is an average of all the trials when a subject was attending stimuli.

In some subjects, a resting baseline will contain a dominant alpha activity spike which is not present in an activity baseline. This is effective when we are determining which stimulus a subject is attending, as opposed to if the subject is attending a stimulus at all.

6.2.6 Statistical Analysis

Once the SNRs for every trial were calculated the data was saved into a 2 dimensional matrix in Matlab. It was done in such a way that a linear mixed-effects model could be fit to the data with function lme from the open source statistical R package nlme. SNRs were modeled as linear functions of the four factors: baseline (activity baseline, closed eyes, open eyes); shape (horizontal lines, horizontal rectangles, squares, vertical rectangles, vertical lines); frequency (8 Hz, 10 Hz, 12Hz, 15Hz, 20 Hz); and electrode placement (PO_7, O_1, O_Z, O_2, PO_8).

Because it was suspected that some of the factors might affect the effect of others, all of their two-way interactions were initially modeled. Since there were 9 subjects whose data varied markedly from each other, the effect of “subject” was included in the model as a random effect, with equal correlations between all pairs of observations from a specific individual. This model is very similar to a linear repeated measures model.

A prerequisite for any linear model is that the data for each stratum come from a population with a normal distribution. As there were only 9 observations in each stratum, a histogram of the combined data was plotted. This showed that the measures were unacceptably skewed for a linear model, so they were log-transformed to obtain a symmetric distribution closer to that of normal. Figure 25 shows the respective histograms.

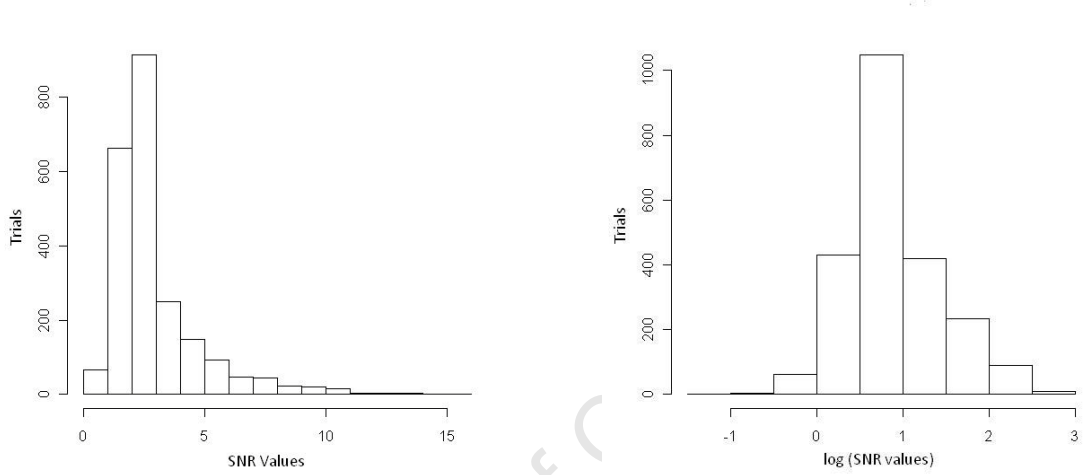

Figure 25. When the total data across all subjects (left) was logged it was found to have a closer to normal distribution (right)

From the ANOVA table of the model, the least significant (largest p-value) interaction was repeatedly selected and removed. This resulted in a model containing terms, all of which contributed independently highly significantly to the model.

When the interactions are examined, the key to finding interaction effects is to observe any non-parallel behavior between the curves representing a particular factor. These will be discussed as they are encountered in section 7.2 and 8.

6.3 Towards a Real-time BCI

Since the ultimate goal of BCI research is to realize a technology that can greatly improve the lives of people living in a locked-in state, it was decided to develop a platform with the open source program Brainbay which can provide a working BCI. Since Brainbay is open source and the modularEEG is inexpensive this can provide researchers with a cheap start to BCI research, as well as a possible cheap solution to encourage more widespread use of BCIs (Wang *et al*, 2008)

Brainbay is written in C++ and is a block-orientated program in which blocks have different functions with which an operator can set up a BCI which processes EEG data in real-time and gives outputs based on the EEG.

The program was initially only able to process time-domain information and provide outputs based on this. For a SSVEP-based BCI data needs to be processed in the frequency domain since the frequency characteristics are relevant to decoding the intentions of the user.

To do this the author fundamentally modified the program, ensuring that data could not only be passed from block to block in single integers but also in arrays of 1 by 512 integers (representing relevant spectral ranges). Functional blocks were also created or altered to accommodate the receiving and manipulation of this 512 integer input. Examples of code written to achieve this can be found in Appendix C.

One application will be described briefly as an example. It was demonstrated at the 2004 Department of Science and Technology Exhibition at the Sandton convention centre. Volunteers were fitted with a headband with 2 active electrodes situated at F_Z and O_Z. They were then presented with two reversing checkerboards at frequencies of 12 and 15Hz on the left and right sides of a bat-ball game on a computer monitor. The object of the game was to prevent the bouncing ball from reaching the bottom of the window by moving a bar left and right by focusing on the left or right stimuli. The setup is illustrated in figure 26.

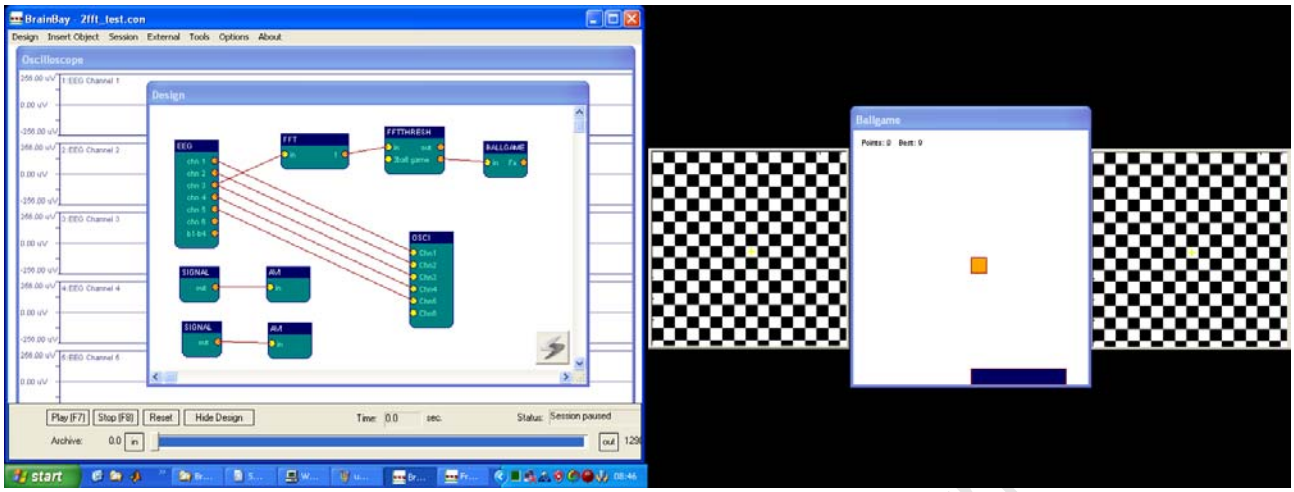

Figure 26. The brainbay setup on the left is made up of functional boxes which are connected by wires. In this way a number of processing algorithms can be programmed independently and then used in series or parallel to test efficacy of individual algorithms or combinations thereof. The author modified the program to enable it to process data in the frequency domain and as such be able to operate as an online SSVEP BCI such as the game on the right hand side and figure 8.

The processing was relatively simple and relied on thresholds of the 12 and 15 Hz bands in the spectrum and producing an output when one of these bands' amplitude exceeded a predefined threshold amplitude (as shown in figure 3). As was also found by Allison *et al* (2010), younger subjects who tested the BCI game at the Exhibition on 2004 were observed to have substantially better success in controlling the movement of the bar.

7 Results

A linear mixed effects model was applied to the logged data as described in section 6.2.6. This was followed by performing a backwards stepwise selection to remove the least significant (highest P-value) interaction and looking at the resulting model. This was repeated until only the significant terms remained. The details of the tables can be found in Appendix D. The ANOVA table of the final model is shown in table 2.

	numDF	denDF	F-value	p-value
(Intercept)	1	2243	81.13	<0.0001
Baseline	2	2243	75.25	<0.0001
Shape	4	2243	13.47	<0.0001
Frequency	4	2243	71.41	<0.0001
Electrode	4	2243	20.54	<0.0001
Baseline:Frequency	8	2243	12.64	<0.0001
Baseline:Electrode	8	2243	2.87	0.0036
Shape:Frequency	16	2243	4.67	<0.0001

Table 2. ANOVA table for final model

All statistical models enable one to predict effects. In this case the prediction of each factor is known as the mean, which is stripped of (co-varied, adjusted, corrected for) all the other factors in the model.

The model first predicts the random effect inter- and intra-subject variances which were found to be 0.29 and 0.39 respectively.

The fixed effect estimation from the model is summarized table 3. Referring to the first column, the first row shows the estimates for the combined means for reference levels of activity baseline, horizontal lines shape, 10 Hz frequency and electrode O_1. They are all therefore part of the intercept value of 0.901. All the other rows are the difference in means (of log(ratio)) from the reference for each estimated effect.

	Value	Std.Error	DF	t-value	p-value
(Intercept)	0.901	0.114	2243	7.88	5.07E-15
Baseline closed_eyes	-0.396	0.065	2243	-6.129	1.04E-09
Baseline open_eyes	-0.154	0.065	2243	-2.381	1.74E-02
Shape horizontal_rectangles	-0.14	0.058	2243	-2.411	1.60E-02
Shape square_checks	0.155	0.059	2243	2.612	9.07E-03
Shape vertical_lines	-0.164	0.058	2243	-2.826	4.76E-03
Shape vertical_rectangles	0.11	0.06	2243	1.833	6.69E-02
Frequency 12_Hz	-0.037	0.07	2243	-0.523	6.01E-01
Frequency 15_Hz	-0.031	0.069	2243	-0.446	6.55E-01
Frequency 20_Hz	0.028	0.069	2243	0.399	6.90E-01
Frequency 8_Hz	0.117	0.069	2243	1.695	9.01E-02
Electrode O2	0.12	0.046	2243	2.603	9.31E-03
Electrode Oz	0.189	0.045	2243	4.158	3.33E-05
Electrode PO7	0.021	0.054	2243	0.386	7.00E-01
Electrode PO8	-0.08	0.052	2243	-1.555	1.20E-01
Baseline closed_eyes:Frequency 12_Hz	0.332	0.065	2243	5.151	2.82E-07
Baseline open_eyes:Frequency 12_Hz	0.244	0.065	2243	3.775	1.64E-04
Baseline closed_eyes:Frequency 15_Hz	0.473	0.064	2243	7.369	2.40E-13
Baseline open_eyes:Frequency 15_Hz	0.322	0.064	2243	5.016	5.69E-07
Baseline closed_eyes:Frequency 20_Hz	0.003	0.064	2243	0.054	9.57E-01
Baseline open_eyes:Frequency 20_Hz	-0.021	0.064	2243	-0.331	7.41E-01
Baseline closed_eyes:Frequency 8_Hz	0.369	0.064	2243	5.743	1.05E-08
Baseline open_eyes:Frequency 8_Hz	0.273	0.064	2243	4.245	2.28E-05
Baseline closed_eyes:Electrode O2	-0.159	0.064	2243	-2.48	1.32E-02
Baseline open_eyes:Electrode O2	-0.268	0.064	2243	-4.183	2.98E-05
Baseline closed_eyes:Electrode Oz	-0.074	0.063	2243	-1.187	2.35E-01
Baseline open_eyes:Electrode Oz	-0.197	0.063	2243	-3.137	1.73E-03
Baseline closed_eyes:Electrode PO7	-0.139	0.075	2243	-1.843	6.55E-02
Baseline open_eyes:Electrode PO7	-0.22	0.075	2243	-2.93	3.43E-03
Baseline closed_eyes:Electrode PO8	-0.033	0.071	2243	-0.459	6.47E-01
Baseline open_eyes:Electrode PO8	-0.088	0.071	2243	-1.236	2.16E-01
Shape horizontal_rectangles:Frequency 12_Hz	0.205	0.083	2243	2.462	1.39E-02
Shape square_checks:Frequency 12_Hz	0.1	0.084	2243	1.192	2.33E-01
Shape vertical_lines:Frequency 12_Hz	0.182	0.083	2243	2.179	2.94E-02
Shape vertical_rectangles:Frequency 12_Hz	0.099	0.085	2243	1.167	2.43E-01
Shape horizontal_rectangles:Frequency 15_Hz	0.059	0.082	2243	0.721	4.71E-01
Shape square_checks:Frequency 15_Hz	-0.092	0.083	2243	-1.106	2.69E-01
Shape vertical_lines:Frequency 15_Hz	-0.017	0.082	2243	-0.208	8.36E-01
Shape vertical_rectangles:Frequency 15_Hz	-0.164	0.083	2243	-1.962	4.99E-02
Shape horizontal_rectangles:Frequency 20_Hz	0.166	0.083	2243	2.013	4.43E-02
Shape square_checks:Frequency 20_Hz	-0.213	0.083	2243	-2.554	1.07E-02
Shape vertical_lines:Frequency 20_Hz	0.197	0.083	2243	2.39	1.69E-02
Shape vertical_rectangles:Frequency 20_Hz	-0.135	0.084	2243	-1.612	1.07E-01
Shape horizontal_rectangles:Frequency 8_Hz	-0.01	0.082	2243	-0.122	9.03E-01
Shape square_checks:Frequency 8_Hz	-0.097	0.083	2243	-1.173	2.41E-01
Shape vertical_lines:Frequency 8_Hz	0.245	0.082	2243	2.978	2.93E-03
Shape vertical_rectangles:Frequency 8_Hz	0.004	0.083	2243	0.052	9.59E-01

Table 3. Summary of fixed effect estimates from final model.

For example, the activity baseline by itself is predicted ("estimated effect") to have a logged ratio of 0.901. An open eyes baseline is predicted to have a logged ratio of 0.747 (0.901-0.154). This is the "intercept" value of 0.901 in table 3 plus the "Baseline open_eyes" difference value in the third line of -0.154 (see table 4 for verification). This open eyes baseline estimate is only for when all three the other the factors are at their baseline values.

If one were to calculate the prediction for the frequency of 12 Hz and the shape "square checks", the intercept value would have the following added to it: difference value of "Frequency 12_Hz" (-0.037); difference value of "Shape square_checks" (0.155); and difference value of "Shape square_checks:Frequency 12_Hz" (0.1). It would be 0.901-0,037+0.155+0.1 = 1.119 (see table 12 for verification).

The 2nd column in Table 3 gives the standard error of the estimate. The next two columns show the degrees of freedom and the t-test on which the p-value is based. The effect sizes can be used to fit or predict the mean log(ratio) for any combination of factor levels.

7.1 Main Effects

Please note that Std.Error, DF, t-value and p-value are "difference effects" related to the "difference values" in table 3, and are included in tables 4 through to 7 only as an indication of the relative effects of the differences. They do not relate linearly to the calculated values in the first column.

7.1.1 Baselines

Baseline	Value	Std.Error	DF	t-value	p-value
Activity baseline	0.901	0.114	2243	7.88	5.07E-15
Open eyes baseline	0.747	0.065	2243	-2.381	1.74E-02
Closed eyes baseline	0.504	0.065	2243	-6.129	1.04E-09

Table 4. Predicted values of the baselines when effects of all other factors have been stripped away. Activity baseline is predicted to have the superior SNR.

The activity baseline was predicted to have a greater SNR than the other baselines as shown in table 4. These estimated means are only for the situation where all other factors are at their reference levels.

7.1.2 Shapes

Of the shapes, the checks had the highest prediction at 1.055 followed by the vertical rectangles at 1.010. The shape predicted to have the lowest SNR is the vertical lines.

A factor which may have an influence on these results is the adaptation and fatigue characteristic discussed in section 4.3. Despite measures being taken to avoid adaptation in terms of relating duration of stimuli to previous literature (Heinrich and Bach, 2001; Beverina *et al*, 2003), it is very difficult to completely understand the effects on such little information. In this case, the vertical lines shape was the trial 21 to 25 in the sequence of trials and also has the smallest predicted SNR, which may indicate an adaptation effect.

Shape	Value	Std.Error	DF	t-value	p-value
Checks	1.055	0.059	2243	2.612	9.07E-03
Vertical rectangles	1.01	0.06	2243	1.833	6.69E-02
Horizontal lines	0.901	0.114	2243	7.88	5.07E-15
Horizontal rectangles	0.761	0.058	2243	-2.411	1.60E-02
Vertical lines	0.737	0.058	2243	-2.826	4.76E-03

Table 5. Predicted values of the shapes when effects of all other factors have been stripped away. Vertical rectangles follows checks as the 2nd highest predicted SNR.

7.1.3 Electrodes

The superior electrode was O_Z at 1.089 with O_2 following with a predicted value of1.021. This result confirms the literature as described in section 4.4. Of interest is that PO_8 is predicted to have the smallest SNR, whereas Beverina *et al* (2003) found it to have the greatest amplitude. As was mentioned in section 4.4. however, the finding of Beverina *et al* was not found to be repeated in other research. There is reason to support activity reported in the areas of PO_8 and PO_7 though as can be seen by the PET activity in figure 13, but it is not supported by this data set.

Electrode	Value	Std.Error	DF	t-value	p-value
Electrode O_Z	1.089	0.045	2243	4.158	3.33E-05
Electrode O_2	1.021	0.046	2243	2.603	9.31E-03
Electrode PO_7	0.922	0.054	2243	0.386	7.00E-01
Electrode O_1	0.901	0.114	2243	7.88	5.07E-15
Electrode PO_8	0.821	0.052	2243	-1.555	1.20E-01

Table 6. Predicted values of the electrodes when effects of all other factors have been stripped away. O_Z which is situated over the primary visual cortex had the highest estimated SNR.

7.1.4 Frequency

8Hz was the frequency of choice at 1.018. 12 and 15 Hz were predicted to have the lowest 2 SNRs. These results support the literature discussed in section 4.1.1. and figure 14 (Regan, 1989). 12 Hz and 15 Hz are between the low and medium frequency ranges as described by Regan and would therefore be expected to have low amplitude. Since the SNRs for all frequencies were calculated over the same frequency range of noise (8 to 30 Hz), the SNR can be seen to be proportional to amplitude. Furthermore, the 2nd harmonics and subharmonic (in the 20 Hz case) used in the SNR are also expected to have higher amplitudes for 8, 10 and 20 Hz than those of 12 and 15 Hz according to figure 14.

Frequency	Value	Std.Error	DF	t-value	p-value
8 Hz	1.018	0.069	2243	1.695	9.01E-02
20 Hz	0.929	0.069	2243	0.399	6.90E-01
10 Hz	0.901	0.114	2243	7.88	5.07E-15
15 Hz	0.87	0.069	2243	-0.446	6.55E-01
12 Hz	0.864	0.07	2243	-0.523	6.01E-01

Table 7. Predicted values of the frequencies when effects of all other factors have been stripped away.

7.2 Interaction Effects

7.2.1 Baseline:Frequency Interaction

The interaction effect in the linear mixed effects model is most pronounced when the respective curves deviate from a parallel behavior as occurred markedly at 10 and 20 Hz in figure 27. The closed-eyes and open-eyes baseline follow each other in a parallel fashion but drop tremendously at 10 and 20Hz. The activity baseline is relatively stable across the frequencies. A comparison for the 10 Hz deviation to figure 24 reveals a similar trend where the closed-eyes and open-eyes baselines show a pronounced alpha spike while the activity baseline has a relatively stable power spectrum. The 20 Hz deviation in figure 27 can be similarly compared to figure 24 because the calculation of the SNR for 20 Hz includes the addition of the power at its subharmonic 10 Hz.

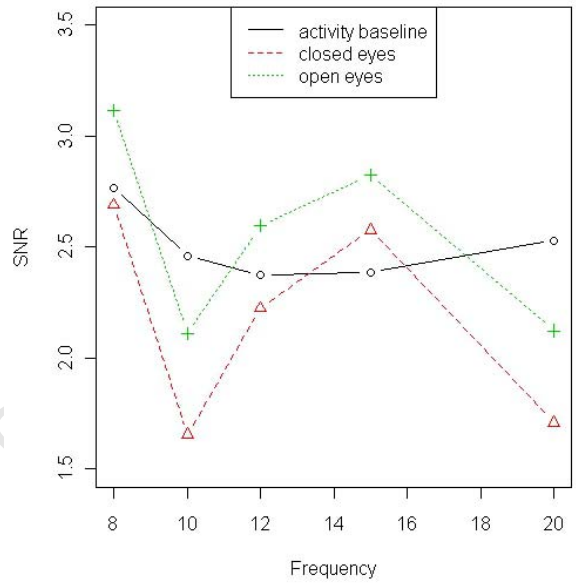

Figure 27. The activity baseline will perform better at 10 and 20 Hz

The values calculated from table 3 were as per the method described in section 6.2.6. The logged values are shown in table 8. These values were then logged to get the values for figure 27. These figures are tabulated in table 9.

	8 Hz	10 Hz	12 Hz	15 Hz	20 Hz
Activity baseline	1.02	0.90	0.86	0.87	0.93
Closed eyes	0.99	0.50	0.80	0.95	0.54
Open eyes	1.14	0.75	0.95	1.04	0.75

Table 8. Logged values showing the individual interaction SNRs of frequency and baseline where all effects of other factors have been stripped away

	8 Hz	10 Hz	12 Hz	15 Hz	20 Hz
Activity baseline	2.77	2.46	2.37	2.39	2.53
Closed eyes	2.69	1.66	2.23	2.58	1.71
Open eyes	3.12	2.11	2.60	2.82	2.12

Table 9. Unlogged values showing the individual interaction SNRs of frequency and baseline

7.2.2 Baseline:Electrode Interaction

The only marked non-parallel behavior is at O_1 where the activity baseline deviates from the others (figure 28). A better understanding of this interaction effect would require further study since there

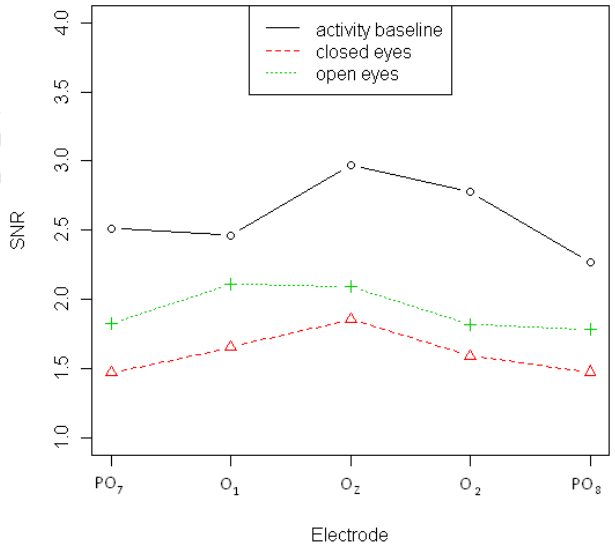

Figure 28. The predicted values expect the activity baseline to perform better across all electrodes, while the eyes-closed baseline is expected to perform the worst.

The activity baseline is a new concept and there is no literature or findings to support this deviation at the specific electrode position. The logged values relating to figure 28 are found in table 10 and the unlogged values in table 11.

	PO_7	O_1	O_Z	O_2	PO_8
Activity baseline	0.92	0.90	1.09	1.02	0.82
Closed eyes	0.39	0.50	0.62	0.47	0.39
Open eyes	0.60	0.75	0.74	0.60	0.58

Table 10. Logged values showing the individual interaction SNRs of electrode and baseline where all effects of other factors have been stripped away

	PO_7	O_1	O_Z	O_2	PO_8
Activity baseline	2.51	2.46	2.97	2.77	2.27
Closed eyes	1.47	1.66	1.86	1.59	1.48
Open eyes	1.83	2.11	2.09	1.82	1.78

Table 11. Unlogged values showing the individual interaction SNRs of electrode and baseline

7.2.3 Shape:Frequency Interaction

A notable deviation from parallel occurs at 8 and 20 Hz for different shapes (figure 29), which is incidentally close to the peaks of the low and middle frequency bands described in figure 14.

In figure 29 the check stimulus has a relatively negative trend when move towards either 8 Hz or 20 Hz from the in between frequencies, while all the other shapes have a positive trend. The shapes appear to be relatively parallel at 10, 12 and 15 Hz.

This interaction effect may indicate that the curves in figure 14 may have different gradients for different stimuli shapes. For instance, for the checks (which as a main effect were predicted to have the greatest SNR) might have flatter curves with less deviation in amplitude across frequencies, while the other shapes might have sharper curves. The concept is illustrated in figure 30. Further investigation is needed to ascertain if this concept fits.

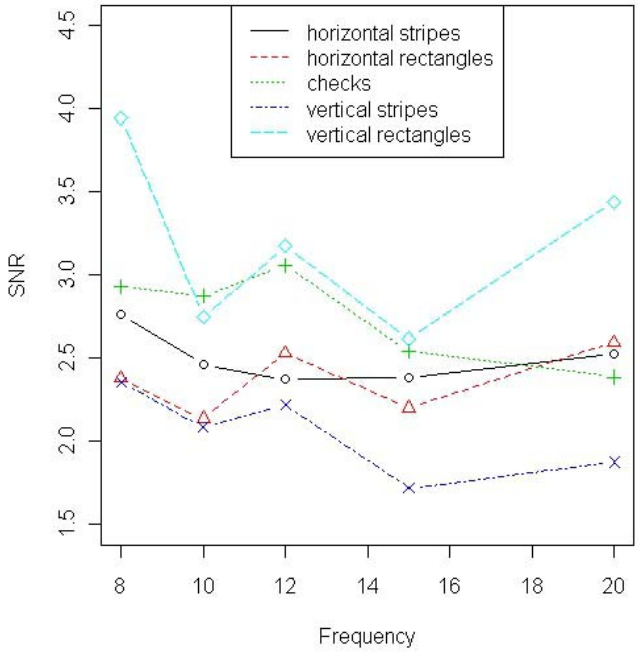

Figure 29. Different shapes over frequency reveal that vertical rectangles are expected to perform best over the majority of the frequencies

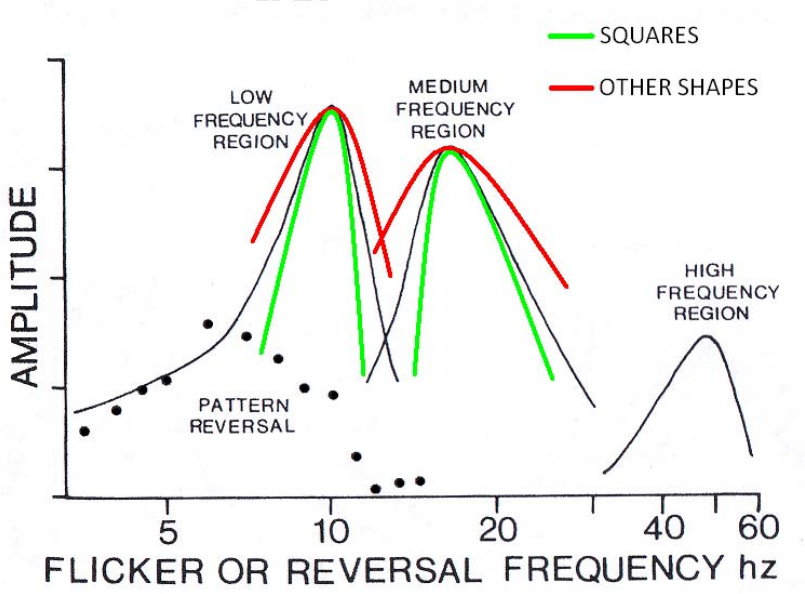

Figure 30. Illustration of concept that may describe the interaction between Frequency and Shapes

Table 12 and 13 show the logged and unlogged values respectively for calculating figure 29.

	8 Hz	10 Hz	12 Hz	15 Hz	20 Hz
Horizontal lines	1.02	0.90	0.86	0.87	0.93
Horizontal rectangles	0.87	0.76	0.93	0.79	0.95
Checks	1.07	1.06	1.12	0.93	0.87
Vertical lines	0.86	0.74	0.80	0.54	0.63
Vertical rectangles	1.37	1.01	1.16	0.96	1.24

Table 12. Logged values showing the individual interaction SNRs of frequency and shape where all effects of other factors have been stripped away

	8 Hz	10 Hz	12 Hz	15 Hz	20 Hz
Horizontal lines	2.77	2.46	2.37	2.39	2.53
Horizontal rectangles	2.38	2.14	2.53	2.20	2.60
Checks	2.93	2.87	3.06	2.54	2.39
Vertical lines	2.36	2.09	2.22	1.72	1.88
Vertical rectangles	3.94	2.75	3.17	2.62	3.44

Table 13. Unlogged values showing the individual interaction SNRs of frequency and shape

8 Discussion

8.1 Main Effects

8.1.1 Activity Baseline

The activity baseline has been proven to be more effective in achieving a high signal to noise ratio for feature extraction. This is a novel finding.

The author believes that the alpha attenuation investigated by Mulholland and Peper (1971) is the difference between the efficacy of an open-eyes resting baseline and an activity baseline. The fact that occipital alpha activity is known to be greater when a subject is not attending a visual stimulus suggests that any baseline other than one linked to visual activity does not in fact reflect a baseline in the context of SSVEP BCIs. Because different subjects' alpha bands are found at different frequencies, even if such a baseline were to be used it would need to be trained to each subject and the stimulation frequencies would need to be outside of the subject-specific alpha band. A activity baseline BCI could present a BCI which does not require subject-specific training.

Furthermore, due to changing EEG over time (Wolpaw *et al*, 2002) a BCI which does not adapt will not operate optimally over time. An "activity baseline" feature extraction method can be a moving-average real-time process that will not require a BCI user to repeatedly record baselines to be effective. This lends itself to a BCI more suited to changing EEG environments with no training requirements.

It must be noted that the activity baseline is best suited to a BCI which is operating at all times because it has excluded the rest mode. Optimal use of such a baseline would be for a BCI user to have an on/off stimulus based on a resting baseline at a frequency outside of the alpha band. This on/off stimulus would be used to put the BCI into or out of "activity mode" where the activity baseline could be used.

An activity baseline is more suited to multiple stimuli because the fewer the stimuli, the larger the averaged peaks are at the various stimulation frequencies as alluded to in figure 24. This could counter the notion expressed by Zhu *et al* (2010) that a high number of targets decreases classifier accuracy and speed.

A further improvement to an activity baseline could be to interpolate over the stimulation frequency peaks mentioned in figure 24. Since the peaks are known to be activity-related artefacts, there should be no negative effects to interpolating between adjacent frequency bands.

8.1.2 Shapes

If vertical line as a shape of stimulus were to be excluded due to possible adaptation or fatigue effects, the predicted SNRs of the different shapes will have been found to follow the trend of the V4 neuron discharge rates for different shaped visual stimuli as shown in figure 12 in chapter 3. As found for single neurons, the checked stimulus responded with the best SNR. The vertical rectangles were similarly the second highest.

The effect of adaptation could be verified if the experiment were to be repeated with a long duration time gap between different shapes, or a change in sequence of the shape stimuli.

8.1.3 Electrodes

The electrode effects found that O_Z expected the highest SNR. This is to be expected since it is situated directly over the primary visual cortex where much visual processing occurs (see chapter 3). In contrast to Beverina *et al* (2003) finding that PO_8 elicited the greatest amplitude over a number of subjects and frequencies, PO_8 was in this case predicted to achieve the smallest SNR of the electrodes tested (discussed in 7.1.3.)

8.1.4 Frequencies

As discussed in 7.1.4., 8 Hz and 20 Hz are close to the peaks of the low and medium frequency bands (see figure 14) which would explain their superior predicted SNRs. The SNRs in this case are proportional to amplitude since they are all calculated from the same frequency range of 8 to 30 Hz. The 20Hz SNR is further strengthened in this case since it is also made up of a 10 Hz subharmonic which also has a relatively high amplitude according to figure 14.

8.2 Interaction Effects

8.2.1 Baseline:Frequency Interaction

The baseline-frequency interaction more clearly shows where with respect to frequency the failure of the traditional open-eyes baseline occurs. The 10 Hz and 20 Hz frequencies both have the amplitude of 10 Hz as a contributing effect to the SNR.

Following on from section 8.1.1., with the alpha band having been recognized historically as very good for SSVEPs, the activity baseline presents the solution to now fully utilize this band for a BCI user.

8.2.2 Baseline:Electrode Interaction

With the frequency and shape effects stripped away, the baseline-electrode interaction again shows the superiority of using an activity baseline for all electrodes tested. Further investigation is needed to ascertain the reason for the effect at O_1 as reported in section 7.2.2.

8.2.3 Shape:Frequency Interaction

Once again the 8 Hz and 20 Hz peaks appear as frequencies with higher SSVEP SNRs which verifies Regan (1989) in figure 14. As discussed in section 7.2.3., the shapes other than the checks have an upward trend at 8 Hz and 20 Hz which may mean that figure 14 changes as suggested in figure 30 depending on the shape of the stimulus. Furthermore, the vertical rectangle shape has the highest predicted value at 4 of the 5 frequencies when the measure is stripped of baseline and electrode effects.

Bibliography

Allison, B., Sugiarto, I., Graimann, B., & Gräser, A. (2008). Display optimization in SSVEP BCIs. *Computer-Human Interaction,*

Allison, B., Luth, T., Valbuena, D., Teymourian, A., Volosyak, I., & Graeser, A. (2010). BCI demographics: How many (and what kinds of) people can use an SSVEP BCI? *IEEE Transactions on Neural Systems and Rehabilitation Engineering : A Publication of the IEEE Engineering in Medicine and Biology Society,*

Allison, B. Z., McFarland, D. J., Schalk, G., Zheng, S. D., Jackson, M. M., & Wolpaw, J. R. (2008). Towards an independent brain-computer interface using steady state visual evoked potentials. *Clinical Neurophysiology : Official Journal of the International Federation of Clinical Neurophysiology, 119*(2), 399-408.

Allison, B. Z., & Pineda, J. A. (2003). ERPs evoked by different matrix sizes: Implications for a brain computer interface (BCI) system. *IEEE Transactions on Neural Systems and Rehabilitation Engineering : A Publication of the IEEE Engineering in Medicine and Biology Society, 11*(2), 110-113.

Arakawa, K., Tobimatsu, S., Tomoda, H., Kira, J., & Kato, M. (1999). The effect of spatial frequency on chromatic and achromatic steady-state visual evoked potentials. *Clinical Neurophysiology : Official Journal of the International Federation of Clinical Neurophysiology, 110*(11), 1959-1964.

Bakardjian, H., Tanaka, T., & Cichocki, A. (2009). Optimization of SSVEP brain responses with application to eight-command brain-computer interface. *Neuroscience Letters,*

Bayliss, J. D. (2003). Use of the evoked potential P3 component for control in a virtual apartment. *IEEE Transactions on Neural Systems and Rehabilitation Engineering : A Publication of the IEEE Engineering in Medicine and Biology Society, 11*(2), 113-116.

BCI2000, " Image:ElectrodePositions 1020.PNG " http://www.bci2000.org/wiki/index.php/Image:ElectrodePositions1020.PNG, 10 February 2010

Beverina, F., Palmas, G., Silvoni, S., Piccione, F., & Giove, S. (2003). User adaptive BCIs: SSVEP and P300 based interfaces. *PsychNology Journal, 1*(4), 331-354.

Birbaumer, N., Ghanayim, N., Hinterberger, T., Iversen, I., Kotchoubey, B., Kubler, A., et al. (1999). A spelling device for the paralysed. *Nature, 398*(6725), 297-298.

Birbaumer, N., Hinterberger, T., Kubler, A., & Neumann, N. (2003). The thought-translation device (TTD): Neurobehavioral mechanisms and clinical outcome. *IEEE Transactions on Neural Systems and Rehabilitation Engineering : A Publication of the IEEE Engineering in Medicine and Biology Society, 11*(2), 120-123.

Blankertz, B., Dornhege, G., Schafer, C., Krepki, R., Kohlmorgen, J., Muller, K. R., et al. (2003). Boosting bit rates and error detection for the classification of fast-paced motor commands based on single-trial EEG analysis. *IEEE Transactions on Neural Systems and Rehabilitation Engineering : A Publication of the IEEE Engineering in Medicine and Biology Society, 11*(2), 127-131.

Cheng, M., Gao, X., Gao, S., & Xu, D. (2002). Design and implementation of a brain-computer interface with high transfer rates. *IEEE Transactions on Bio-Medical Engineering, 49*(10), 1181-1186.

Dechent, P., Merboldt, K. D., & Frahm, J. (2004). Is the human primary motor cortex involved in motor imagery? *Brain Research.Cognitive Brain Research, 19*(2), 138-144.

Fukunaga, K. (1990). *Introduction to statistical pattern recognition* Academic Pr.

Gao, X., Xu, D., Cheng, M., & Gao, S. (2003). A BCI-based environmental controller for the motion-disabled. *IEEE Transactions on Neural Systems and Rehabilitation Engineering : A Publication of the IEEE Engineering in Medicine and Biology Society, 11*(2), 137-140.

Guger, C., Daban, S., Sellers, E., Holzner, C., Krausz, G., Carabalona, R., et al. (2009). How many people are able to control a P300-based brain–computer interface (BCI)? *Neuroscience Letters, 462*(1), 94-98.

Heinrich, S. P., & Bach, M. (2001). Adaptation dynamics in pattern-reversal visual evoked potentials. *Documenta Ophthalmologica.Advances in Ophthalmology, 102*(2), 141-156.

Heinrich, S. P., & Bach, M. (2003). Adaptation characteristics of steady-state motion visual evoked potentials. *Clinical Neurophysiology : Official Journal of the International Federation of Clinical Neurophysiology, 114*(7), 1359-1366.

Hillyard, S. A., Hinrichs, H., Tempelmann, C., Morgan, S. T., Hansen, J. C., Scheich, H., et al. (1997). Combining steady-state visual evoked potentials and fMRI to localize brain activity during selective attention. *Human Brain Mapping, 5*(4), 287-292.

Kandel, E. R., Schwartz, J. H., & Jessell, T. M. (2000). *Principles of neural science* McGraw-Hill/Appleton & Lange.

Kelly, S. P., Lalor, E. C., Reilly, R. B., & Foxe, J. J. (2005). Visual spatial attention tracking using high-density SSVEP data for independent brain-computer communication. *IEEE Transactions on Neural Systems and Rehabilitation Engineering : A Publication of the IEEE Engineering in Medicine and Biology Society, 13*(2), 172-178.

Leeb, R., Friedman, D., Muller-Putz, G. R., Scherer, R., Slater, M., & Pfurtscheller, G. (2007). Self-paced (asynchronous) BCI control of a wheelchair in virtual environments: A case study with a tetraplegic. *Computational Intelligence and Neuroscience,* , 79642.

Loki23, "An Idiots Guide to Dreaming" http://loki23.blogspot.com/2009/09/10-20-neurobasment.html; 23 January 2010

Lyskov, E., Ponomarev, V., Sandstrom, M., Mild, K. H., & Medvedev, S. (1998). Steady-state visual evoked potentials to computer monitor flicker. *International Journal of Psychophysiology : Official Journal of the International Organization of Psychophysiology, 28*(3), 285-290.

Mackay, A. M., Bradnam, M. S., & Hamilton, R. (2003). Rapid detection of threshold VEPs. *Clinical Neurophysiology : Official Journal of the International Federation of Clinical Neurophysiology, 114*(6), 1009-1020.

Middendorf, M., McMillan, G., Calhoun, G., & Jones, K. S. (2000). Brain-computer interfaces based on the steady-state visual-evoked response. *IEEE Transactions on Rehabilitation Engineering : A Publication of the IEEE Engineering in Medicine and Biology Society, 8*(2), 211-214.

Millan Jdel, R., & Mourino, J. (2003). Asynchronous BCI and local neural classifiers: An overview of the adaptive brain interface project. *IEEE Transactions on Neural Systems and Rehabilitation Engineering : A Publication of the IEEE Engineering in Medicine and Biology Society, 11*(2), 159-161.

Morgan, S. T., Hansen, J. C., & Hillyard, S. A. (1996). Selective attention to stimulus location modulates the steady-state visual evoked potential. *Proceedings of the National Academy of Sciences of the United States of America, 93*(10), 4770-4774.

Muhl, C., Gurkok, H., Bos, O., Thurlings, M., Scherffig, L., Duvinage, M., et al. (2010). Bacteria hunt: A multimodal, multiparadigm BCI game.

Mukesh, T. M. S., Jaganathan, V., Reddy, M. R. (2006). A novel multiple frequency stimulation method for steady state VEP based brain computer interfaces. Physiol. Meas. 27, 61-71.

Mulholland, T. B., & Peper, E. (1971). Occipital alpha and accommodative vergence, pursuit tracking, and fast eye movements. *Psychophysiology, 8*(5), 556-575.

Müller, M. M., Picton, T. W., Valdes-Sosa, P., Riera, J., Teder-Sälejärvi, W. A., & Hillyard, S. A. (1998). Effects of spatial selective attention on the steady-state visual evoked potential in the 20–28 hz range. *Cognitive Brain Research, 6*(4), 249-261.

Muller, M. M., & Hubner, R. (2002). Can the spotlight of attention be shaped like a doughnut? evidence from steady-state visual evoked potentials. *Psychological Science : A Journal of the American Psychological Society / APS, 13*(2), 119-124.

Muller, R., Gopfert, E., Breuer, D., & Greenlee, M. W. (1998). Motion VEPs with simultaneous measurement of perceived velocity. *Documenta Ophthalmologica.Advances in Ophthalmology, 97*(2), 121-134.

Muller-Putz, G. R., Scherer, R., Brauneis, C., & Pfurtscheller, G. (2005). Steady-state visual evoked potential (SSVEP)-based communication: Impact of harmonic frequency components. *Journal of Neural Engineering, 2*(4), 123-130.

Müller-Putz, G. R., Eder, E., Wriessnegger, S. C., & Pfurtscheller, G. (2008). Comparison of DFT and lock-in amplifier features and search for optimal electrode positions in SSVEP-based BCI. *Journal of Neuroscience Methods, 168*(1), 174-181.

Neuper, C., & Pfurtscheller, G. (2001). Evidence for distinct beta resonance frequencies in human EEG related to specific sensorimotor cortical areas. *Clinical Neurophysiology : Official Journal of the International Federation of Clinical Neurophysiology, 112*(11), 2084-2097.

Niedermeyer, E., & Da Silva, F. H. L. (2004). *Electroencephalography: Basic principles, clinical applications, and related fields* Lippincott Williams & Wilkins.

Nielsen, K. D., Cabrera, A. F., & do Nascimento, O. F. (2006). EEG based BCI-towards a better control. brain-computer interface research at aalborg university. *IEEE Transactions on Neural Systems and Rehabilitation Engineering, 14*(2), 202.

Nijboer, F., Sellers, E. W., Mellinger, J., Jordan, M. A., Matuz, T., Furdea, A., et al. (2008). A P300-based brain–computer interface for people with amyotrophic lateral sclerosis. *Clinical Neurophysiology, 119*(8), 1909-1916.

Nikondigital.org, http://www.nikondigital.org/dps/images/HVS-web.jpg, 10 February 2010

Parra, L. C., Spence, C. D., Gerson, A. D., & Sajda, P. (2003). Response error correction--a demonstration of improved human-machine performance using real-time EEG monitoring. *IEEE Transactions on Neural Systems and Rehabilitation Engineering : A Publication of the IEEE Engineering in Medicine and Biology Society, 11*(2), 173-177.

Pfurtscheller, G., Muller, G. R., Pfurtscheller, J., Gerner, H. J., & Rupp, R. (2003). 'Thought'--control of functional electrical stimulation to restore hand grasp in a patient with tetraplegia. *Neuroscience Letters, 351*(1), 33-36.

Pfurtscheller, G., & Neuper, C. (1997). Motor imagery activates primary sensorimotor area in humans. *Neuroscience Letters, 239*(2-3), 65-68.

Pfurtscheller, G., Neuper, C., & Krausz, G. (2000). Functional dissociation of lower and upper frequency mu rhythms in relation to voluntary limb movement. *Clinical Neurophysiology : Official Journal of the International Federation of Clinical Neurophysiology, 111*(10), 1873-1879.

Piccione, F., Giorgi, F., Tonin, P., Priftis, K., Giove, S., Silvoni, S., et al. (2006). P300-based brain computer interface: Reliability and performance in healthy and paralysed participants. *Clinical Neurophysiology, 117*(3), 531-537.

Poulin, Francois. The agony of old concepts. 19 June 2008. http://drfpoulin.wordpress.com/2008/06/19/the-agony-of-old-concepts/. 10 February 2010

Prueckl, R., & Guger, C. (2009). A brain-computer interface based on steady state visual evoked potentials for controlling a robot. *Proceedings of the 10th International Work-Conference on Artificial Neural Networks: Part I: Bio-Inspired Systems: Computational and Ambient Intelligence,* 697.

Schalk, G., Wolpaw, J. R., McFarland, D. J., & Pfurtscheller, G. (2000). EEG-based communication: Presence of an error potential. *Clinical Neurophysiology, 111*(12), 2138-2144.

Sutter, E.E. (1992). The brain response interface communication through visually induced electrical brain response, *J. Microcomp. Appl.*, 15, 31-45.

Teplan, M. (2002). Fundamentals of EEG measurement. *Measurement Science Review, 2*(2), 1-11.

Trejo, L. J., Rosipal, R., & Matthews, B. (2006). Brain-computer interfaces for 1-D and 2-D cursor control: Designs using volitional control of the EEG spectrum or steady-state visual evoked

potentials. *IEEE Transactions on Neural Systems and Rehabilitation Engineering : A Publication of the IEEE Engineering in Medicine and Biology Society, 14*(2), 225-229.

Vialatte, F. B., Maurice, M., Dauwels, J., & Cichocki, A. (2009). Steady-state visually evoked potentials: Focus on essential paradigms and future perspectives. *Progress in Neurobiology,*

Wang, Y., Wang, R., Gao, X., Hong, B., & Gao, S. (2006). A practical VEP-based brain-computer interface. *IEEE Transactions on Neural Systems and Rehabilitation Engineering, 14*(2), 234-240.

Wang, Y., Wang, R., Gao, X., Hong, B., & Gao, S. (2006). A practical VEP-based brain-computer interface. *IEEE Transactions on Neural Systems and Rehabilitation Engineering, 14*(2), 234-240.

Wang, Y., Zhang, Z., Gao, X., & Gao, S. (2004). Lead selection for SSVEP-based brain-computer interface. *Proceedings of the 26th Annual Meeting of IEEE EMBS,* 4507–4510.

Wang, H., & Zheng, W. (2008). Local temporal common spatial patterns for robust single-trial EEG classification. *IEEE Transactions on Neural Systems and Rehabilitation Engineering : A Publication of the IEEE Engineering in Medicine and Biology Society, 16*(2), 131-139.

Wills, S. A., & MacKay, D. J. (2006). DASHER--an efficient writing system for brain-computer interfaces? *IEEE Transactions on Neural Systems and Rehabilitation Engineering : A Publication of the IEEE Engineering in Medicine and Biology Society, 14*(2), 244-246.

Wolpaw, J. R., Birbaumer, N., McFarland, D. J., Pfurtscheller, G., & Vaughan, T. M. (2002). Brain–computer interfaces for communication and control. *Clinical Neurophysiology, 113*(6), 767-791.

Wu, Z., Lai, Y., Xia, Y., Wu, D., & Yao, D. (2008). Stimulator selection in SSVEP-based BCI. *Medical Engineering & Physics, 30*(8), 1079-1088.

Wu, Z., & Yao, D. (2008). Frequency detection with stability coefficient for steady-state visual evoked potential (SSVEP)-based BCIs. *Journal of Neural Engineering, 5*(1), 36-43.

Zhu, D., Bieger, J., Molina, G. G., & Aarts, R. M. (2010). A survey of stimulation methods used in SSVEP-based BCIs.

APPENDIX A: ELECTRODES

Numerous types of electrodes were built and tested. The most simple of these were passive electrodes made from Silver (Ag) wires. The wires were used as placed in a 1:50 HCl solution and a current was passed through them for 5 minutes. Each electrode was then inserted into a slit in a sponge wet with a KCl solution and attached to the author's scalp by holding it in place with an elastic band around the head. The electrode and sponge are shown in Figure A1.

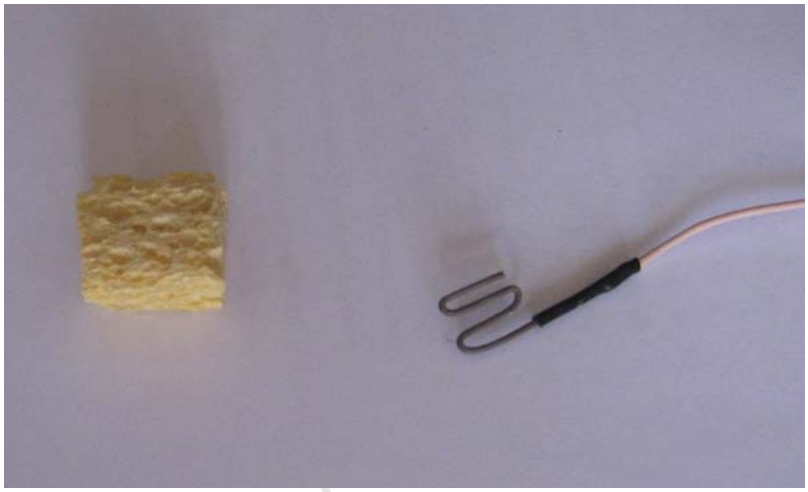

Figure A1. AgCl electrode with sponge

Since the process of preparing a subject was a bit cumbersome with this setup, easier to use electrodes were developed using ECG electrodes.

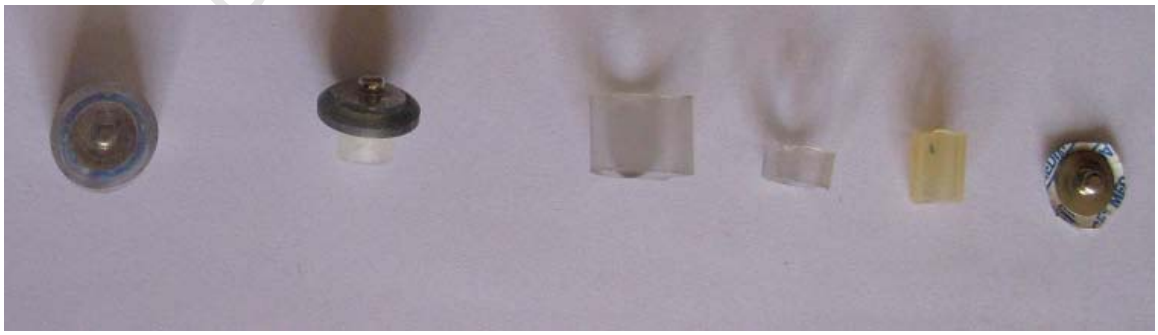

Figure A2. The components used with an ECG disc used to make a passive electrode

The AgCl disc of ECG electrodes were cut out and put inside a short piece of silicon tubing of inside diameter equal to the outside diameter of the AgCl disc. This was secured in place by 2 2mm long pieces of silicon tubing of same outer diameter as the AgCl disc. See figure A2.

A headband as seen in figure 21 with silicon tube holes was made such that the silicon tubing was of inner diameter equal to the outer diameter of the outer electrode tube. When the electrode was inserted into this hole it fitted snuggly and did not move at all. To ensure electrical contact with the scalp, EEG paste was inserted into the scalp side of the electrode. This proved to be very practical and easy to put on a subject. It still showed pronounced movement related artifacts, partly due to the fact that the back of the ECG AgCl was connected to the lead by a button clip. Since EEG activity is 10^3 order of magnitude smaller than that of ECG, the connection has to be far superior for transmission of all signals.

Active electrodes were subsequently built since they had promise to simplify the setup further (no paste or salt solution necessary) (see figure A3). They would also reduce movement related noise because there is a unity gain amplifier at the electrode itself.

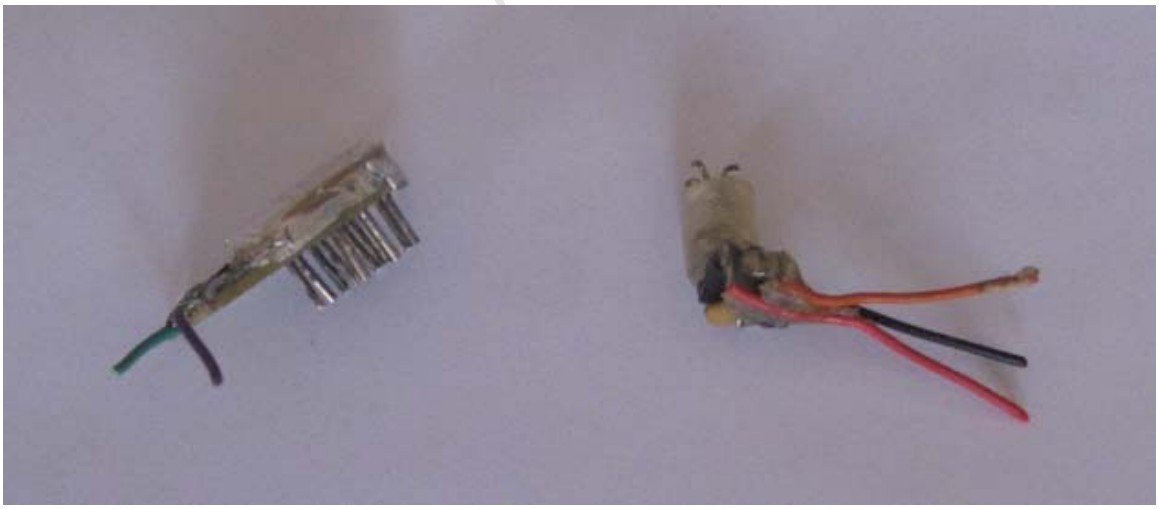

Figure A3. An electrode with spikes (left) allows the scalp to be reached through hair. The active electrode (right) has wires for power and the signal.

In principle, an active electrode works in a capacitive way. A suitable element (in this case Ag) is placed against the scalp and experiences current flow as a result of the electromagnetic forces created by

current flow in the scalp just beneath it. The unity gain amplifier drives this signal to the amplifier for further amplification. This type of electrode was used with success at the 2004 Department of Science and Technology Exhibition in Sandton. Subjects would sit in a chair looking at a computer monitor and have the headband put on. F_Z and O_Z were the only 2 electrodes, F_Z being a flat stripe of Ag which made contact with the skin on the forehead, and O_Z was a specially 2D comb-shaped electrode of Ag wires designed to gain access through the hair to the scalp.

APPENDIX B: MATLAB CODE

The Matlab code was summarized in figure 22 and is reproduced in figure B2. What follows is excerpts of code to give the reader insight into how the outcomes were achieved. Matlab 6.5 (R13) was used.

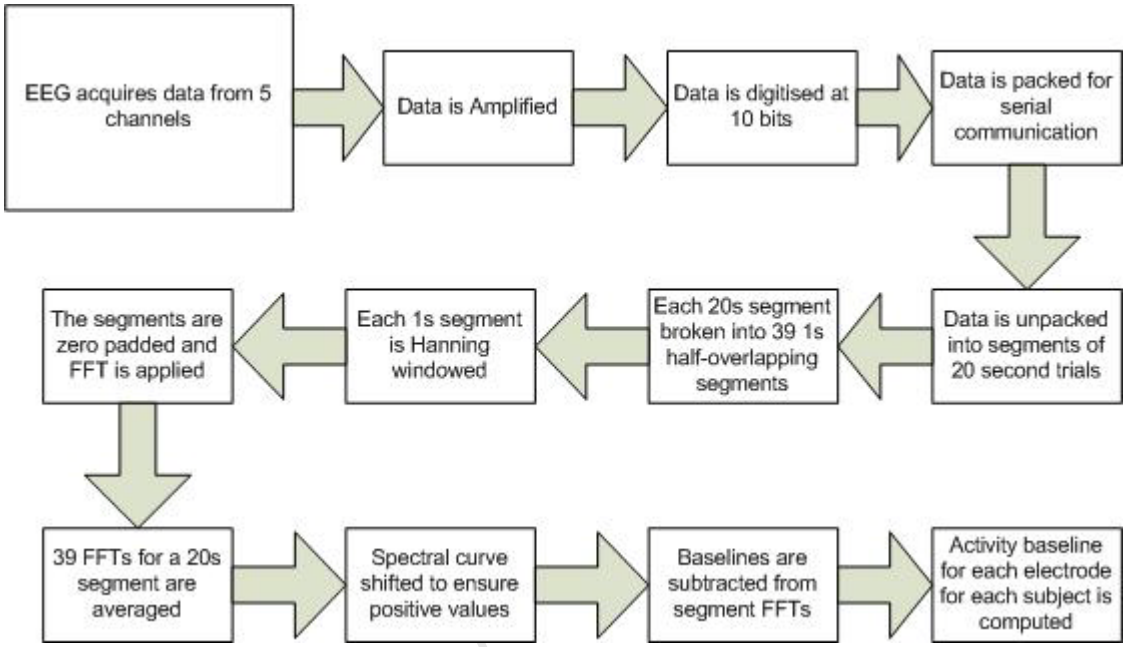

Figure B2. Flow diagram for Matlab code

Following will be code describing particular blocks in figure B2 and parts thereof.

The following code was written by Angel Lin, a former MSc student. It **unpacks the data** received from the modularEEG and saves it as a .mat file. It describes the following block:

```
clear all;
tic
fid = fopen('Subject1.arc');

ch1_vector = [];
ch2_vector = [];
ch3_vector = [];
ch4_vector = [];
ch5_vector = [];
ch6_vector = [];
```

```
[test1_header, count]=fread(fid,255,'uint8');

 for loop = 1:11
   [test1_data, count] = fread(fid,1,'uint8');
   if test1_data >= 128
              break;
   end
 end

%for data_size = 1:inf       % 76800 = 300secs

   [data1, count]=fread(fid,inf,'uint8');     %read the whole file into data1
 m = max(size(data1))
for k = 1:11:(m - 11)
      test1_data = data1(k:k+10);
      C = bitget(test1_data(5),7:-1:5);
   ch1_sample = C(1)*2^10 + C(2)*2^9 + C(3)*2^8 + test1_data(3);
   C = bitget(test1_data(5),3:-1:1);
   ch2_sample = C(1)*2^10 + C(2)*2^9 + C(3)*2^8 + test1_data(4);
   C = bitget(test1_data(8),7:-1:5);
   ch3_sample = C(1)*2^10 + C(2)*2^9 + C(3)*2^8 + test1_data(6);
  C = bitget(test1_data(8),3:-1:1);
   ch4_sample = C(1)*2^10 + C(2)*2^9 + C(3)*2^8 + test1_data(7);
   C = bitget(test1_data(11),7:-1:5);
   ch5_sample = C(1)*2^10 + C(2)*2^9 + C(3)*2^8 + test1_data(9);

   C = bitget(test1_data(11),3:-1:1);
   ch6_sample = C(1)*2^10 + C(2)*2^9 + C(3)*2^8 + test1_data(10);
   ch1_vector = [ch1_vector ch1_sample];
   ch2_vector = [ch2_vector ch2_sample];
   ch3_vector = [ch3_vector ch3_sample];
    ch4_vector = [ch4_vector ch4_sample];
   ch5_vector = [ch5_vector ch5_sample];
   ch6_vector = [ch6_vector ch6_sample];

    if bitget(test1_data(11),8) == 1

     else
       break;
   end

 j = j +1;
```

```
end

epoch_vector = zeros(1,j);
for i = 181:100:j

if (ch6_vector(i) > ch6_vector(i-100) + 200) | (ch6_vector(i) < ch6_vector(i-100) - 200)
   epoch_vector(i) = 1;

end
end

eeglab1 = [ch1_vector;ch2_vector;ch3_vector;ch4_vector;ch5_vector;epoch_vector];

fclose(fid)
toc
t = toc
save Subject1.mat
```

This data was then broken into the relevant epochs using the EEGlab tool for Matlab and saved into .set files for each subject.

The following code takes all the data in these individual files and **puts them into a structure array** called m(subjectnumber).

```
cd('C:\MATLAB6p5\work\data\subject6');
[ALLEEG EEG CURRENTSET ALLCOM] = eeglab;
EEG = pop_loadset('sub6ch_4_40_27_20sec_epochs.set');
[ALLEEG EEG CURRENTSET] = eeg_store(ALLEEG,EEG);
for i = 1:max(size(EEG.event))
   [EEG1,eventindices] = pop_selectevent(EEG, 'epoch', i);
   x = ['sub6epoch',int2str(i),'_20sec.set'];
   pop_saveset(EEG1, x);
end
m(6)=ALLEEG;
```

The data was then hanning windowed and FFT'd as follows:

```
clear all;
load('C:\MATLAB6p5\work\data\total_data.mat','m');
```

```
for n=1:9                                                    %test subject number 1 to 9
  for k=1:27                                                 %trial number 1 to 27
    for j=1:5                                                %electrode number 1 to 5
      FFT_accumulator = zeros(1,512);                        %FFT_accumulator accumulates all the 1 second FFTs during 1 trial
      for i=0:38                                             %39 1 second data windows, half overlapped, over 20 seconds
        w = hann(256);                                       %Hanning window over the 1 second window
        Y = fft(m(n).data(j,(i*128)+1:(i+2)*128,k).*w',512); %FFT of 1 second window for subject and trial and 1 second window iteration
        Pyy = Y.* conj(Y) / 512;                             %Obtain Power Spectrum
        FFT_accumulator = FFT_accumulator + Pyy;             %FFT_accumulator accumulates all the 1 second FFTs during 1 trial
      end                                                    %end 1 second window iteration
      FFT_average = FFT_accumulator/39;                      %FFT_average gets average FFT over the 20 second trial
      Master_matrix(n,k,j,1:512) = FFT_average;              %Master_matrix stores all FFTs of all subjects, trials and electrodes
    end                                                      %end electrode iteration
  end                                                        %end trial iteration
end                                                          %end subject iteration
```

The data was then put into a 5 dimensional matrix:

```
%The following script splits the 1:27 trials per subject of Master_matrix into a
%7X6 array where the first 5X5 are the 5 shapes by the 5 frequencies, (6,6) is
%eyes closed baseline, and (7,6) eyes open baseline.
%SpectrumMatrix is 5D of size (9,7,6,5,512) relating to (Subject, shape, freq, electrode, spectrum)

SpectrumMatrix(:,1,1:5,:,:) = Master_matrix(:,2:6,:,:);    %Assign horizontal lines at freq 8 - 20 to SpectrumMatrix(:,1,1:5,:,:)
SpectrumMatrix(:,2,1:5,:,:) = Master_matrix(:,7:11,:,:);   %Assign horizontal rectangles at freq 8 - 20 to SpectrumMatrix(:,2,1:5,:,:)
SpectrumMatrix(:,3,1:5,:,:) = Master_matrix(:,12:16,:,:);  %Assign checks at freq 8 - 20 to SpectrumMatrix(:,3,1:5,:,:)
SpectrumMatrix(:,4,1:5,:,:) = Master_matrix(:,17:21,:,:);  %Assign vertical rectangles and freq 8 - 20 to SpectrumMatrix(:,4,1:5,:,:)
SpectrumMatrix(:,5,1:5,:,:) = Master_matrix(:,22:26,:,:);  %Assign vertical lines and freq 8 - 20 to SpectrumMatrix(:,5,1:5,:,:)
SpectrumMatrix(:,6,6,:,:) = Master_matrix(:,1,:,:);        %Eyes closed baseline (at freq 0) to SpectrumMatrix(:,6,6,:,:)
SpectrumMatrix(:,7,6,:,:) = Master_matrix(:,27,:,:);       %Eyes open baseline (at freq 0) to SpectrumMatrix(:,7,6:5,:,:)

save('C:\MATLAB6p5\work\data\Master_power_spectrum.mat','SpectrumMatrix');
```

The 3 baselines are then calculated and bad electrodes and omitted trial were excluded.

```
%getting the eyes closed, eyes open, and activity baseline saved as
%baseline_matrix size (9,3,5,512) for subject, baseline number (1 = eyes
%closed; 2 = eyes open; 3 = activity baseline), electrode, spectrum points.
%the activity baseline is the average of the 25 events of each subject.
clear all;
load('C:\MATLAB6p5\work\data\Master_power_spectrum.mat','SpectrumMatrix');
%accumulatingbaseline1 = zeros(1,512);
```

```
for o=1:9
   totalbaseline1 = zeros(1,512);
   for p=1:5
      for s=1:512
         baseline_matrix(o,1,p,s) = SpectrumMatrix(o,6,6,p,s);
      end
   end
end
for o=1:9
   for p=1:5
      totalbaseline3 = zeros(1,512);
      for q=1:5
         if o==1                    %taking out dodgy electrodes on some subjects and trials where electrodes were not working
            if p==1|p==2|p==5
               break
            end
         end


            accumulatingbaseline3(1,s) = SpectrumMatrix(o,q,r,p,s);
         end
         totalbaseline3 = totalbaseline3 + accumulatingbaseline3;
      end
   end
   if o==1|o==8
      baseline_matrix(o,3,p,:) = totalbaseline3/24;
   elseif o==2
      baseline_matrix(o,3,p,:) = totalbaseline3/23;
   else
      baseline_matrix(o,3,p,:) = totalbaseline3/25;
   end
  end
end
save('C:\MATLAB6p5\work\data\Baseline_spectrum.mat','baseline_matrix');
```

The baseline spectra are then subtracted from each trial spectrum

```
%puts the data in a 9X375 array (SNRarray) of baselined SNR points of order
%baseline, shape, frequency, electrode (3X5X5X5 = 375) for ANOVA
%baselinedarray is 9X375X512 of the Spectrum matrix minus the baselines
clear all;
load('C:\MATLAB6p5\work\data\Baseline_spectrum.mat','baseline_matrix');
load('C:\MATLAB6p5\work\data\Master_power_spectrum.mat','SpectrumMatrix');
```

```
for o=1:9
  for q=1:5
    for r=1:5
      for p=1:5
        for s=1:512
          baselinedarray(o,(q-1)*25+(r-1)*5+p,s) = (SpectrumMatrix(o,q,r,p,s)-baseline_matrix(o,1,p,s));%/baseline_matrix(o,1,p,s)+1;
        end
      end
    end
  end
end
```

And the **baseline offset is taken away by moving the smallest SNR** between 8 Hz and 40 Hz to 0 and the rest of the spedtrum by the same margin.

```
for o=1:9
  for t=0:5:74
    for u=1:5
        baselinedarray(o,5*(t+3)+u,:)=baselinedarray(o,5*(t+3)+u,:)-min(baselinedarray(o,5*(t+3)+u,16:80));
      SNRarray(o,5*(t+3)+u) = (baselinedarray(o,5*(t+3)+u,30)+baselinedarray(o,5*(t+3)+u,60))/mean(baselinedarray(o,5*(t+3)+u,16:80));
    end
  end
end
```

And finally, the data is **transformed into a 2D array as required by R**.

```
lme_array(2:376,1) = cellstr('subject_1');
lme_array(2+(375*1):376+(375*1),1) = cellstr('subject_2');
lme_array(2+(375*2):376+(375*2),1) = cellstr('subject_3');
lme_array(2+(375*3):376+(375*3),1) = cellstr('subject_4');
lme_array(2+(375*4):376+(375*4),1) = cellstr('subject_5');
lme_array(2+(375*5):376+(375*5),1) = cellstr('subject_6');
lme_array(2+(375*6):376+(375*6),1) = cellstr('subject_7');
lme_array(2+(375*7):376+(375*7),1) = cellstr('subject_8');
lme_array(2+(375*8):376+(375*8),1) = cellstr('subject_9');

for x=0:8
  lme_array(2+(375*x):126+(375*x),2) = cellstr('open_eyes');
  lme_array(127+(375*x):251+(375*x),2) = cellstr('closed_eyes');
```

```
   lme_array(252+(375*x):376+(375*x),2) = cellstr('activity_baseline');
end

for y=0:26
   lme_array(2+(125*y):26+(125*y),3) = cellstr('horizontal_lines');
   lme_array(27+(125*y):51+(125*y),3) = cellstr('horizontal_rectangles');
   lme_array(52+(125*y):76+(125*y),3) = cellstr('square_checks');
   lme_array(77+(125*y):101+(125*y),3) = cellstr('vertical_rectangles');
   lme_array(102+(125*y):126+(125*y),3) = cellstr('vertical_lines');
end

for z=0:134
   lme_array(2+(25*z):6+(25*z),4) = cellstr('8_Hz');
   lme_array(7+(25*z):11+(25*z),4) = cellstr('10_Hz');
   lme_array(12+(25*z):16+(25*z),4) = cellstr('12_Hz');
   lme_array(17+(25*z):21+(25*z),4) = cellstr('15_Hz');
   lme_array(22+(25*z):26+(25*z),4) = cellstr('20_Hz');
end

for a=0:674
   lme_array(2+(5*a),5) = cellstr('PO7');
   lme_array(3+(5*a),5) = cellstr('O3');
   lme_array(4+(5*a),5) = cellstr('Oz');
   lme_array(5+(5*a),5) = cellstr('O4');
   lme_array(6+(5*a),5) = cellstr('PO8');
end

for v=2:376
   for w=0:8
      lme_array(w*375+v,6) = num2cell(abs(SNRarray(w+1,v-1)));       %3375X6:  ID, baseline, shape, frequency, electrode, 6 and its absolute
   end
end
lme_array(1,1:6) = [cellstr('Subject') cellstr('Baseline') cellstr('Shape') cellstr('Frequency') cellstr('Electrode') cellstr('Ratio')];
xlswrite('c:\lme_array7.xls', lme_array);
```

APPENDIX C: C++ WORK

The crux of the work was transforming the open source program Brainbay from one that operates only in the time domain to one operating also in the frequency domain. This allows the application of a BCI using the frequency domain, provided the objects are written. The author also wrote some frequency domain objects including a correlation object which differentiated between 12 and 15 Hz stimuli for a SSVEP BCI.

To achieve the frequency domain functionality, the object “base” had to be altered. Base controls the movement of data from one object to another. “Linkfft” was created to allow the movement of a 512 word structure from object to object.

```
#define MAX_CONNECTS 40
#define MAX_OBJECTS 150

void report_error( char * Message );
extern class BASE_CL * objects[MAX_OBJECTS];
extern class BASE_CL * actobject;


typedef struct LINKStruct
{
   int from_port;
            int to_object;
            int to_port;
} LINKStruct ;

class BASE_CL
{
 public:
            int type;
            int inports;
            int outports;
            int xPos;
            int yPos;
            int width;
            int height;
            HWND displayWnd;
```

```
        char in_name[MAX_CONNECTS][17];
        char out_name[MAX_CONNECTS][17];

        LINKStruct  out[MAX_CONNECTS];
  HWND hDlg;

        BASE_CL (void)
        {
                int i;
                width=0; height=0; displayWnd=NULL;
                for (i=0;i<MAX_CONNECTS;i++) { in_name[i][0]=0; out_name[i][0]=0; }
        }
        virtual ~BASE_CL (void) {}
        virtual void work (void) {}
        virtual void make_dialog (void) {}
        virtual void load (HANDLE hFile) {}
        virtual void save (HANDLE hFile) {}
        virtual void incoming_data(int port, float value) {}
        virtual void incoming_datafft(int portfft, float valuefft[512]) {}

        void pass_values (int port, float value)
        {
                LINKStruct * act_link;
                for (act_link=&(out[0]);act_link->to_port!=-1;act_link++)
                        if (act_link->from_port==port)
                                objects[act_link->to_object]->incoming_data(act_link->to_port, value);
        }

        void pass_valuesfft (int portfft, float valuefft[512])
                {
                        LINKStruct * act_linkfft;
                        for (act_linkfft=&(out[0]);act_linkfft->to_port!=-1;act_linkfft++)
                                if (act_linkfft->from_port==portfft)
                                        objects[act_linkfft->to_object]->incoming_datafft(act_linkfft->to_port, valuefft);
                }
};
```

The Correlation Object is as follows:

```
#include "brainbay.h"
#include "ob_fftcorrelation.h"
#include <iostream>
```

```
#include <cmath>

using namespace std;

CORRELATIONFFTOBJ::CORRELATIONFFTOBJ(int num) : BASE_CL()
{
		outports = 1;
		inports = 2;
		width=100;
		strcpy(out_name[0],"out");
  accum1 = 0.0;
  accum2 = 0.0;
  for (int i = 0; i < NUMSAMPLES; i++)
  {
		samples1[i] = 0.0;
    samples2[i] = 0.0;
  }
		for (int j = 0; j < 512; j++)
  {
		corr_fft_out[j] = 0.0;
  }
  //interval = 1;
  writepos1 = 0;
  writepos2 = 0;
  added1 = 0;
  added2 = 0;
		fftbuff = 1;
}

void CORRELATIONFFTOBJ::make_dialog(void)
{
		//display_toolbox(hDlg=CreateDialog(hInst, (LPCTSTR)IDD_CORRFFTBOX, ghWndMain, (DLGPROC)CorrfftDlgHandler));
}

void CORRELATIONFFTOBJ::load(HANDLE hFile)
{
		load_property("xpos",P_INT,&xPos);
		load_property("ypos",P_INT,&yPos);
  //load_property("interval",P_INT,&interval);
}

void CORRELATIONFFTOBJ::save(HANDLE hFile)
{
```

```
		save_property(hFile,"xpos",P_INT,&xPos);
		save_property(hFile,"ypos",P_INT,&yPos);
  //save_property(hFile,"interval",P_INT,&interval);
}

void CORRELATIONFFTOBJ::incoming_data(int port, float value) {}

void CORRELATIONFFTOBJ::incoming_datafft(int portfft, float value[512])
{
		//if (portfft == 0)
		//		input1 = value;
		//else if (portfft == 1)
		//		input2 = value;

		for (int i = 0; i < 512; i++)
		{
		float *accum, *samples;
  int *writepos, *added;
		switch (portfft)
  {
		case 0:
		accum = &accum1;
	samples = samples1;
	writepos = &writepos1;
	added = &added1;
		break;
    case 1:
		accum = &accum2;
	samples = samples2;
	writepos = &writepos2;
	added = &added2;
		break;
    default:
		return;
  }
		samples[*writepos] = value[i];
		(*accum) += value[i];
  (*added)++;
  if ((*added) > 10)//interval)
  {
		int oldest = (*writepos) - 10;//interval;
		if (oldest < 0)
			oldest += NUMSAMPLES;
```

```
                (*accum) -= samples[oldest];
        (*added) = 10;//interval;
    }
                (*writepos)++;
    if ((*writepos) >= NUMSAMPLES)
                (*writepos) = 0;
                }
}

void CORRELATIONFFTOBJ::work(void)
{
                float *corr_fft_out;
                //int *fftbuff;
                float mean1 = accum1 / added1;
    float mean2 = accum2 / added2;

    float C12 = 0, V1 = 0, V2 = 0;
    int pos1 = writepos1;
    int pos2 = writepos2;
    int added = (added1 < added2)?added1:added2;
    for (int i = 0; i < added; i++)
    {
                float diff1 = samples1[pos1] - mean1;
        float diff2 = samples2[pos2] - mean2;
        C12 += diff1 * diff2;
        V1 += diff1 * diff1;
        V2 += diff2 * diff2;

        pos1--;
        pos2--;
        if (pos1 < 0)
                pos1 = NUMSAMPLES - 1;
        if (pos2 < 0)
                pos2 = NUMSAMPLES - 1;
    }

    C12 /= 10;//interval;
    V1 /= 10;//interval;
    V2 /= 10;//interval;
    float correlation = C12 / sqrt(V1 * V2);
                corr_fft_out[fftbuff] = correlation;

                if (fftbuff > 510)
```

```
		{
			pass_valuesfft(0, corr_fft_out);
			fftbuff = 0;
		}
		else
			fftbuff++;

}
```

APPENDIX D: R CODE

The data read into R was of the following format:

Subject ID	Baseline	Shape	Frequency	Electrode	Ratio
subject_4	activity_baseline	vertical_lines	15_Hz	PO_8	2.460495
subject_4	activity_baseline	vertical_lines	20_Hz	PO_7	2.669406
subject_4	activity_baseline	vertical_lines	20_Hz	O_1	0.907732
subject_4	activity_baseline	vertical_lines	20_Hz	O_Z	1.555307
subject_4	activity_baseline	vertical_lines	20_Hz	O_2	2.307647
subject_4	activity_baseline	vertical_lines	20_Hz	PO_8	2.899346
subject_5	open_eyes	horizontal_lines	8_Hz	PO_7	2.301057
subject_5	open_eyes	horizontal_lines	8_Hz	O_1	3.209551
subject_5	open_eyes	horizontal_lines	8_Hz	O_Z	3.732595
subject_5	open_eyes	horizontal_lines	8_Hz	O_2	3.537321

Table D1. Format of data read into R

The properties were as shown in table D2:

Subject	Baseline	Shape	Frequency	Electrode	Ratio
subject_1: 375	activity_baseline:1125	horizontal_lines: 675	10_Hz:675	O_1 :675	Min. : 0.33
subject_2: 375	closed_eyes: 1125	horizontal_rectangles: 675	12_Hz:675	O_2 :675	1st Qu.: 1.79
subject_3: 375	open_eyes: 1125	square_checks: 675	15_Hz:675	O_Z :675	Median : 2.21
subject_4: 375		vertical_lines: 675	20_Hz:675	PO_7:675	Mean : 2.84
subject_5: 375		vertical_rectangles: 675	8_Hz :675	PO_8:675	3rd Qu.: 3.26
subject_6: 375					Max. : 15.28
(Other) :1125					NA's :1077.00

Table D2. Properties of data read into R

A linear mixed effects operation was performed on the data, after which an anova was performed. The results are shown in table D3.

	numDF	denDF	F-value	p-value
(Intercept)	1	2203	81.32	<.0001
Baseline	2	2203	75.51	<.0001
Shape	4	2203	13.52	<.0001
Frequency	4	2203	71.66	<.0001
Electrode	4	2203	20.62	<.0001
Baseline:Shape	8	2203	1.47	0.1641
Baseline:Frequency	8	2203	12.75	<.0001
Baseline:Electrode	8	2203	2.88	0.0034
Shape:Frequency	16	2203	4.69	<.0001
Shape:Electrode	16	2203	0.80	0.6854
Frequency:Electrode	16	2203	1.42	0.1233

Table D3. Initial ANOVA table

This ANOVA table was then reduced to Table 2 as discussed in the Results section.

The R code following reads the required data, applies a linear mixed effects (lme) model to the log of the data, and repeatedly performs ANOVAs while remove insignificant interactions.

```
Data1=read.table("lme_array9.txt",sep="\t",header=T)
summary(Data1)

modn = lme(log(Ratio)~(Baseline+Shape+Frequency+Electrode)^2, data=Data1,random=~1|Subject, na.action=na.exclude)
anova(modn)

modn=update(modn,.~.-Shape:Electrode)
anova(modn)
modn=update(modn,.~.-Baseline:Shape)
anova(modn)
modn=update(modn,.~.-Frequency:Electrode)
anova(modn)

summary(modn)$tTable
```

The following code builds the table for the Baseline:Frequency interaction plot based on the summary table 3 in the Results.

```
%Baseline vs Frequency
baseline_frequency_matrix = matrix(nrow=5,ncol=3)
baseline_frequency_matrix[1,1]=summary(modn)$tTable[1,1]+summary(modn)$tTable[11,1]
baseline_frequency_matrix[2,1]=summary(modn)$tTable[1,1]
baseline_frequency_matrix[3,1]=summary(modn)$tTable[1,1]+summary(modn)$tTable[8,1]
baseline_frequency_matrix[4,1]=summary(modn)$tTable[1,1]+summary(modn)$tTable[9,1]
baseline_frequency_matrix[5,1]=summary(modn)$tTable[1,1]+summary(modn)$tTable[10,1]
baseline_frequency_matrix[1,2]=summary(modn)$tTable[1,1]+summary(modn)$tTable[11,1]+summary(modn)$tTable[2,1]+summary(modn
)$tTable[22,1]
baseline_frequency_matrix[2,2]=summary(modn)$tTable[1,1]+summary(modn)$tTable[2,1]
baseline_frequency_matrix[3,2]=summary(modn)$tTable[1,1]+summary(modn)$tTable[8,1]+summary(modn)$tTable[2,1]+summary(modn)
$tTable[16,1]
baseline_frequency_matrix[4,2]=summary(modn)$tTable[1,1]+summary(modn)$tTable[9,1]+summary(modn)$tTable[2,1]+summary(modn)
$tTable[18,1]
baseline_frequency_matrix[5,2]=summary(modn)$tTable[1,1]+summary(modn)$tTable[10,1]+summary(modn)$tTable[2,1]+summary(modn
)$tTable[20,1]
baseline_frequency_matrix[1,3]=summary(modn)$tTable[1,1]+summary(modn)$tTable[11,1]+summary(modn)$tTable[3,1]+summary(modn
)$tTable[23,1]
baseline_frequency_matrix[2,3]=summary(modn)$tTable[1,1]+summary(modn)$tTable[3,1]
baseline_frequency_matrix[3,3]=summary(modn)$tTable[1,1]+summary(modn)$tTable[8,1]+summary(modn)$tTable[3,1]+summary(modn)
$tTable[17,1]
baseline_frequency_matrix[4,3]=summary(modn)$tTable[1,1]+summary(modn)$tTable[9,1]+summary(modn)$tTable[3,1]+summary(modn)
$tTable[19,1]
baseline_frequency_matrix[5,3]=summary(modn)$tTable[1,1]+summary(modn)$tTable[10,1]+summary(modn)$tTable[3,1]+summary(modn
)$tTable[21,1]
```

The following code builds the table for the Baseline:Electrode interaction plot based on the summary table 3 in the Results.

```
%Baseline vs Electrode
 = matrix(nrow=5,ncol=3)
baseline_electrode_matrix[1,1]=summary(modn)$tTable[1,1]+summary(modn)$tTable[14,1]
baseline_electrode_matrix[2,1]=summary(modn)$tTable[1,1]
baseline_electrode_matrix[3,1]=summary(modn)$tTable[1,1]+summary(modn)$tTable[13,1]
baseline_electrode_matrix[4,1]=summary(modn)$tTable[1,1]+summary(modn)$tTable[12,1]
baseline_electrode_matrix[5,1]=summary(modn)$tTable[1,1]+summary(modn)$tTable[15,1]
baseline_electrode_matrix[1,2]=summary(modn)$tTable[1,1]+summary(modn)$tTable[14,1]+summary(modn)$tTable[2,1]+summary(modn)
$tTable[28,1]
baseline_electrode_matrix[2,2]=summary(modn)$tTable[1,1]+summary(modn)$tTable[2,1]
baseline_electrode_matrix[3,2]=summary(modn)$tTable[1,1]+summary(modn)$tTable[13,1]+summary(modn)$tTable[2,1]+summary(modn)
$tTable[26,1]
baseline_electrode_matrix[4,2]=summary(modn)$tTable[1,1]+summary(modn)$tTable[12,1]+summary(modn)$tTable[2,1]+summary(modn)
$tTable[24,1]
baseline_electrode_matrix[5,2]=summary(modn)$tTable[1,1]+summary(modn)$tTable[15,1]+summary(modn)$tTable[2,1]+summary(modn)
$tTable[30,1]
baseline_electrode_matrix[1,3]=summary(modn)$tTable[1,1]+summary(modn)$tTable[14,1]+summary(modn)$tTable[3,1]+summary(modn)
$tTable[39,1]
baseline_electrode_matrix[2,3]=summary(modn)$tTable[1,1]+summary(modn)$tTable[3,1]
baseline_electrode_matrix[3,3]=summary(modn)$tTable[1,1]+summary(modn)$tTable[13,1]+summary(modn)$tTable[3,1]+summary(modn)
$tTable[27,1]
baseline_electrode_matrix[4,3]=summary(modn)$tTable[1,1]+summary(modn)$tTable[12,1]+summary(modn)$tTable[3,1]+summary(modn)
$tTable[25,1]
baseline_electrode_matrix[5,3]=summary(modn)$tTable[1,1]+summary(modn)$tTable[15,1]+summary(modn)$tTable[3,1]+summary(modn)
$tTable[31,1]
```

The following code builds the table for the Shape:Frequency interaction plot based on the summary table 3 in the Results

```
%Shape vs frequency
shape_frequency_matrix = matrix(nrow=5,ncol=5)
shape_frequency_matrix[1,1]=summary(modn)$tTable[1,1]+summary(modn)$tTable[11,1]
shape_frequency_matrix[2,1]=summary(modn)$tTable[1,1]
shape_frequency_matrix[3,1]=summary(modn)$tTable[1,1]+summary(modn)$tTable[8,1]
shape_frequency_matrix[4,1]=summary(modn)$tTable[1,1]+summary(modn)$tTable[9,1]
shape_frequency_matrix[5,1]=summary(modn)$tTable[1,1]+summary(modn)$tTable[10,1]
shape_frequency_matrix[1,2]=summary(modn)$tTable[1,1]+summary(modn)$tTable[11,1]+summary(modn)$tTable[4,1]+summary(modn)$tTable[44,1]
shape_frequency_matrix[2,2]=summary(modn)$tTable[1,1]+summary(modn)$tTable[4,1]
shape_frequency_matrix[3,2]=summary(modn)$tTable[1,1]+summary(modn)$tTable[8,1]+summary(modn)$tTable[4,1]+summary(modn)$tTable[32,1]
shape_frequency_matrix[4,2]=summary(modn)$tTable[1,1]+summary(modn)$tTable[9,1]+summary(modn)$tTable[4,1]+summary(modn)$tTable[36,1]
shape_frequency_matrix[5,2]=summary(modn)$tTable[1,1]+summary(modn)$tTable[10,1]+summary(modn)$tTable[4,1]+summary(modn)$tTable[40,1]
shape_frequency_matrix[1,3]=summary(modn)$tTable[1,1]+summary(modn)$tTable[11,1]+summary(modn)$tTable[5,1]+summary(modn)$tTable[45,1]
shape_frequency_matrix[2,3]=summary(modn)$tTable[1,1]+summary(modn)$tTable[5,1]
shape_frequency_matrix[3,3]=summary(modn)$tTable[1,1]+summary(modn)$tTable[8,1]+summary(modn)$tTable[5,1]+summary(modn)$tTable[33,1]
shape_frequency_matrix[4,3]=summary(modn)$tTable[1,1]+summary(modn)$tTable[9,1]+summary(modn)$tTable[5,1]+summary(modn)$tTable[37,1]
shape_frequency_matrix[5,3]=summary(modn)$tTable[1,1]+summary(modn)$tTable[10,1]+summary(modn)$tTable[5,1]+summary(modn)$tTable[41,1]
shape_frequency_matrix[1,4]=summary(modn)$tTable[1,1]+summary(modn)$tTable[11,1]+summary(modn)$tTable[6,1]+summary(modn)$tTable[47,1]
shape_frequency_matrix[2,4]=summary(modn)$tTable[1,1]+summary(modn)$tTable[6,1]
shape_frequency_matrix[3,4]=summary(modn)$tTable[1,1]+summary(modn)$tTable[8,1]+summary(modn)$tTable[6,1]+summary(modn)$tTable[35,1]
shape_frequency_matrix[4,4]=summary(modn)$tTable[1,1]+summary(modn)$tTable[9,1]+summary(modn)$tTable[6,1]+summary(modn)$tTable[39,1]
shape_frequency_matrix[5,4]=summary(modn)$tTable[1,1]+summary(modn)$tTable[10,1]+summary(modn)$tTable[6,1]+summary(modn)$tTable[43,1]
shape_frequency_matrix[1,5]=summary(modn)$tTable[1,1]+summary(modn)$tTable[11,1]+summary(modn)$tTable[7,1]+summary(modn)$tTable[46,1]
shape_frequency_matrix[2,5]=summary(modn)$tTable[1,1]+summary(modn)$tTable[7,1]
shape_frequency_matrix[3,5]=summary(modn)$tTable[1,1]+summary(modn)$tTable[8,1]+summary(modn)$tTable[7,1]+summary(modn)$tTable[34,1]
```

```
shape_frequency_matrix[4,5]=summary(modn)$tTable[1,1]+summary(modn)$tTable[9,1]+summary(modn)$tTable[7,1]+summary(modn)$tTable[38,1]
shape_frequency_matrix[5,5]=summary(modn)$tTable[1,1]+summary(modn)$tTable[10,1]+summary(modn)$tTable[7,1]+summary(modn)$tTable[42,1]
```

Finally, they matrices are plotted

```
%matplot(c(8,10,12,15,20),exp(baseline_frequency_matrix),type="b",xlab="Frequency",ylab="Baselines",pch=1:3,ylim=c(1,4))
%legend("top",legend=c("activity baseline","closed eyes","open eyes"),col=1:3,lty=1:3)
matplot(exp(baseline_electrode_matrix),type="b",xlab="Electrode",ylab="SNR",pch=1:3,ylim=c(1,4))
legend("top",legend=c("activity baseline","closed eyes","open eyes"),col=1:3,lty=1:3)

%matplot(c(8,10,12,15,20),exp(shape_frequency_matrix),type="b",xlab="Frequency",ylab="SNR",pch=1:5,ylim=c(1.5,4.5))
%legend("top",legend=c("horizontal lines","horizontal rectangles","checks","vertical lines","vertical rectangles"),col=1:5,lty=1:5)
```